



Experimental motivation and empirical consistency in minimal no-collapse quantum mechanics

Maximilian Schlosshauer

Department of Physics, University of Washington, Seattle, WA 98195, USA

Received 19 August 2005; accepted 31 October 2005

Available online 15 December 2005

Abstract

We analyze three important experimental domains (SQUIDs, molecular interferometry, and Bose–Einstein condensation) as well as quantum-biophysical studies of the neuronal apparatus to argue that (i) the universal validity of unitary dynamics and the superposition principle has been confirmed far into the mesoscopic and macroscopic realm in all experiments conducted thus far; (ii) all observed “restrictions” can be correctly and completely accounted for by taking into account environmental decoherence effects; (iii) no positive experimental evidence exists for physical state-vector collapse; (iv) the perception of single “outcomes” is likely to be explainable through decoherence effects in the neuronal apparatus. We also discuss recent progress in the understanding of the emergence of quantum probabilities and the objectification of observables. We conclude that it is not only viable, but moreover compelling to regard a minimal no-collapse quantum theory as a leading candidate for a physically motivated and empirically consistent interpretation of quantum mechanics. © 2005 Elsevier Inc. All rights reserved.

PACS: 03.65.Ta; 03.65.Yz; 03.75.–b; 03.75.Gg

Keywords: No-collapse quantum mechanics; Decoherence; Measurement problem; Quantum-to-classical transition; Superposition principle; Entanglement; SQUIDs; Molecular diffraction; Bose–Einstein condensation; Physical collapse theories; Quantum probabilities; Objectification of observables; Neuronal decoherence

E-mail address: MAXL@u.washington.edu

1. Introduction

Historically, quantum theory was motivated by the need to describe the behavior of microscopic systems not explainable by the laws of classical physics. Not only was quantum mechanics deemed unnecessary for a description of the macroworld of our experience, it also led to “strange” consequences that seemed to blatantly contradict our experience, as famously illustrated by the Schrödinger-cat *Gedanken* experiment [1] and later generally referred to as the “measurement problem.” Therefore quantum theory was often, as in the Copenhagen interpretation, banned a priori from the macroscopic realm.

Over the past decade, however, a rapidly growing number of experiments have demonstrated the existence of quantum superpositions of mesoscopically and macroscopically distinct states on increasingly large scales. Such superpositions are observed as individual quantum states and are perfectly explained by unitarily evolving wave functions. On the other hand, decoherence theory [2–7] has enabled one to understand the fragility of such superpositions, and thus the extreme difficulty in observing them outside of sophisticated experimental setups, as being due to ubiquitous quantum interactions with environmental degrees of freedom.

These developments have thus extended the domain for an application of quantum theory far into the mesoscopic and macroscopic realm, which lends strong support to assuming a universally exact and applicable Schrödinger equation. To make a physically compelling case for such a purely unitary quantum theory we must pursue two related goals. First, we ought to continue to design experiments which demonstrate the existence of quantum superpositions of macroscopically distinct states—and which, ideally, can explicitly rule out collapse models. Second, since the assumption of a universal Schrödinger dynamics implies that superpositions of (presumably macroscopically) different observer states are both possible and inescapable if we include physical observers into the quantum-mechanical description, we must simultaneously show that environmental decoherence provides the necessary and sufficient mechanism to explain our observation of a “classical” world. The emergence of the latter can then be understood not only in spite of, but precisely *because* of the quantum formalism—no classical prejudice need to be imposed.

The formal basis for a derivation of a viable interpretation of quantum mechanics from the “bare” unitary formalism alone has been outlined in several papers. The basic idea was introduced in Everett’s proposal of a relative-state view of quantum mechanics [8]. It was later adapted and popularized by DeWitt [9–11] in his “many-worlds” interpretation of quantum mechanics, whose elements go far beyond the abstract sketches of Everett and which must therefore be strictly distinguished from Everett’s proposal [12]. Relative-state interpretations were subsequently fleshed out, by taking into account decoherence effects, in works by Zeh [2,3,13], Zurek [14,5,15], Wallace [16,17], and others (see, for example, [18–20]). Such a theory can be based on the most minimal set of assumptions about the quantum formalism and its interpretation. First, a completely known (pure) state of an isolated quantum system \mathcal{S} is described by a normalized state vector $|\psi\rangle$ in a Hilbert space $H_{\mathcal{S}}$. Second the time evolution of a state vector $|\psi\rangle$ is given by the Schrödinger equation $i\hbar \frac{\partial}{\partial t} |\psi\rangle = \hat{H}_{\mathcal{S}} |\psi\rangle$, where $\hat{H}_{\mathcal{S}}$ is the Hamiltonian of the system \mathcal{S} . No mention is made of measurements in this formulation. Instead, measurements are described without special axioms in terms of physical interactions between systems described by state vectors (wave

functions) and governed by suitable interaction Hamiltonians. Observables then emerge as a derived concept (see, for example, [6,5]).

In this paper, however, we take a less formal route and focus on an analysis of the experimental and theoretical progress (with an emphasis on the former) towards the two goals mentioned before, namely, the continued acquisition of experimental evidence for superpositions of macroscopically distinct states and an explanation for the emergence of definite perceptions in spite of an assumed universal validity of the superposition principle.

Our goal was to show that there is no experimental evidence for a breakdown of the superposition principle and the related interference effects at any length scale investigated thus far. Whenever a decay of such superpositions is observed, it can be fully accounted for (both experimentally and theoretically) as resulting from environmental interactions. The absence of any empirical evidence for nonlinear deviations from unitary time evolution, combined with the ability to give an empirically adequate description of the decoherence of superpositions into apparent mixtures, provides good reasons to take the universal validity of the Schrödinger equation as a working assumption and to explore the consequences of this assumption.

The resulting theory will require more attention to a detailed quantum-mechanical description of observers and observations. Such an account is interpretation-neutral, while the question of its relevance for solving the measurement problem may depend on the particular features of an interpretation. This is so because there exist interpretations, for example, Bohmian mechanics or modal interpretations, that claim to solve the measurement problem *without* having to give an explicit account of the physical processes describing observers and observations (see also Section 3).

This paper is organized as follows. In Section 2, we shall discuss and analyze three important experimental domains—superconducting quantum interference devices (SQUIDs), matter-wave interferometry, and Bose–Einstein condensation—that have provided evidence for superpositions of macroscopically distinguishable states. Section 3 comments on the current status of physical collapse theories in view of the described experiments. In Sections 4 and 5, we shall discuss steps towards the resolution of two issues that have often been considered as posing a challenge to relative-state interpretations: The question of the origin of quantum probabilities and the connection with Born’s rule, and the problem of the “objectification” of observables and thus the emergence of “classical reality.” Section 6 analyzes theoretical models for decoherence in the perceptive and cognitive apparatus, and the implications of such decoherence processes. Finally, in Section 7, we shall summarize our main conclusions and discuss possible next steps.

2. Superpositions of macroscopically distinct states: experiments and implications

In the following, we shall describe three recent experimental areas that have led to (or that are very close to achieving) the observation of superpositions of mesoscopically and macroscopically distinguishable states: Coherent quantum tunneling in SQUIDs (Section 2.2), diffraction of C_{70} (and larger) molecules in matter-wave interferometers (Section 2.3), and number-difference superpositions in two-species Bose–Einstein condensates (Section 2.4). These experiments have achieved the largest such superpositions observed thus far and also represent the most promising experimental domains for achieving even larger superpositions in the future.

For some earlier experiments demonstrating mesoscopic and macroscopic quantum effects, see the setups using superconductors [21–25], nanoscale magnets [26–28], laser-cooled trapped ions [29], and photons in a microwave cavity [30,31]. We would also like to mention Leggett’s review article [32] which discusses some experiments that probe the limits of quantum mechanics. Leggett’s motivation, however, is somewhat different than that of the present author, as Leggett’s main aim is to assess the status of physical collapse theories in view of these experiments.

2.1. *Measuring the macroscopic distinctness of states in a superposition*

Before embarking on an analysis of the experiments, we shall first lend a more precise meaning to the ubiquitous phrase “superposition of macroscopically distinct (or distinguishable) states.” If confronted with a superposition of two states $|A\rangle$ and $|B\rangle$ of the form

$$|\Psi\rangle = \frac{1}{\sqrt{2}}(|A\rangle + |B\rangle), \quad (1)$$

how are we to decide whether this indeed represents a macroscopic Schrödinger-cat state? Clearly, two conditions will need to be fulfilled:

- (1) The states $|A\rangle$ and $|B\rangle$ must differ macroscopically in some extensive quantity (e.g., spatial separation, total mass, magnetic moment, momentum, charge, current, etc.), relative to a suitable microscopic reference value.
- (2) The degree of GHZ-type entanglement [33] in the state $|\Psi\rangle$, i.e., the number of correlations that would need to be measured to distinguish this state from a mixture, must be sufficiently large. With $|A\rangle$ and $|B\rangle$ usually representing GHZ-like multi-particle states in complex systems such as superconducting currents, molecules, and atomic gases, this measure can typically be well-estimated by the number of microscopic constituents (electrons, protons, and neutrons) in the system.

A similar combination of two measures has been suggested by Leggett [34,32] under the labels “extensive difference” and “disconnectivity.” We shall adopt Leggett’s former term for the first condition, and use the term “degree of entanglement” for the second. A both necessary and sufficient condition for a superposition to be considered a superposition of macroscopically distinct states is then given by the requirement that both the extensive difference between $|A\rangle$ and $|B\rangle$ and the interparticle entanglement in $|\Psi\rangle$ be large relative to an appropriate microscopic unit.

2.2. *Superconducting quantum interference devices*

Experiments using SQUIDs have not only demonstrated that the dynamics of a macroscopic quantity of matter (here $\approx 10^9$ Cooper pairs) can be collectively determined by a single macroscopic coordinate governed by quantum mechanics, but have also achieved the creation and indirect observation of quantum superpositions of two truly macroscopic states that correspond to currents of several μA running in opposite directions.

2.2.1. SQUID setup and detection of superpositions of macroscopically distinct currents

A SQUID consists of a superconducting loop interrupted by a Josephson junction and immersed into an external magnetic field that creates a flux Φ_{ext} through the loop. This allows for a persistent dissipationless current (“supercurrent”) to flow around the loop, in clockwise or counterclockwise direction, creating an additional flux. Such a current is composed of a very large number of Cooper pairs (i.e., Bose-condensed electron pairs) whose collective center-of-mass motion can be described by a macroscopic wave function around the loop.

Since the wave function must be continuous around the loop, an integer k times its wavelength must equal the circumference of the loop. Since the Josephson junction induces a discontinuous phase drop $\Delta\phi_J$, and since the total change in phase around the superconducting loop is given by $2\pi\Phi/\Phi_0$, where $\Phi_0 = h/2e$ is the flux quantum and Φ is the total trapped flux through the loop, the phase continuity condition implies

$$\Delta\phi_J + 2\pi\Phi/\Phi_0 = 2\pi k, \quad (2)$$

with $k = 1, 2, \dots$. This means that the collective quantum dynamics of the SQUID are determined by the single macroscopic variable Φ .

The effective SQUID Hamiltonian can be written as [35]

$$\hat{H} = \frac{\hat{P}_\Phi^2}{2C} + U(\Phi) = -\frac{\hbar^2}{2C} \frac{d^2}{d\Phi^2} + \left[\frac{(\Phi - \Phi_{\text{ext}})^2}{2L} - \frac{I_c \Phi_0}{2\pi} \cos\left(2\pi \frac{\Phi}{\Phi_0}\right) \right], \quad (3)$$

where C is the total capacitance (mainly due to the junction), L is the (finite) self-inductance of the loop, and I_c is the critical current of the junction. This Hamiltonian induces dynamics that are analogous to the motion of a particle with effective “mass” C moving in Φ -space in a tilted one-dimensional double-well potential, with the tilt determined by Φ_{ext} . The role of the canonical variables \hat{X} and \hat{P} is here played by the total trapped flux $\hat{\Phi}$ and the total displacement current $\hat{P}_\Phi = -i\hbar d/d\hat{\Phi}$ (which has units of charge; $Cd\hat{P}_\Phi/dt$ is the charge difference across the junction).

A set of eigenstates $|k\rangle$ of the Hamiltonian of Eq. (3), called “ k -fluxoid states,” are localized in one of the wells of the potential below the (classically impenetrable) barrier if the damping induced by the Josephson junction is weak. The corresponding wave functions $\psi_k(\Phi) \equiv \langle \Phi | k \rangle$ are locally s -harmonic, so their amplitudes are peaked around the respective minimum of $U(\Phi)$ with narrow spreads in flux space. Thus, these low-lying energy eigenstates have a relatively small range of associated flux values and can therefore (at least for sufficiently small k) also be viewed as “fuzzy” eigenstates of the flux operator. By adjusting Φ_{ext} , the energy levels are shifted, and for certain values of Φ_{ext} , two levels in opposite wells can be made to align, which allows for resonant quantum tunneling between the wells (i.e., between two fluxoid states) [36,24], leading to a macroscopic change in the magnetic moment of the system.

The most important states for our subsequent treatment are the zero-fluxoid state $|0\rangle$ and the one-fluxoid state $|1\rangle$. Since the states $|0\rangle$ and $|1\rangle$ are localized in, respectively, the left and right well of the potential, let us denote them by $|L\rangle$ and $|R\rangle$ in the following. These states correspond (apart from the quantum zero-point energy [37]) to a classical persistent-current state and thus to macroscopically distinguishable directions of the superconducting current. Since other states are well separated in energy, the SQUID can thus

be effectively modeled as a macroscopic quantum-mechanical two-state system (i.e., as a macroscopic qubit).

At bias $\Phi_{\text{ext}} = \Phi_0/2$, the well becomes symmetric and the corresponding two fluxoid states $|L\rangle$ and $|R\rangle$ would become degenerate (see Fig. 1). However, the degeneracy is lifted by the formation of symmetric and antisymmetric superpositions of $|L\rangle$ and $|R\rangle$ that represent the new energy ground state

$$|\Psi_s\rangle = \frac{1}{\sqrt{2}}(|L\rangle + |R\rangle) \tag{4}$$

with energy E_+ , and the first excited energy eigenstate

$$|\Psi_a\rangle = \frac{1}{\sqrt{2}}(|L\rangle - |R\rangle) \tag{5}$$

with energy E_- . Thus these eigenstates are delocalized across the two wells. The (typically very small) energy splitting $\Delta E = E_a - E_s$ is determined by the WKB matrix elements for tunneling between the two wells (and thus between $|L\rangle$ and $|R\rangle$), and is only dependent on the capacitance C of the junction, scaling as $\Delta E \propto e^{-\sqrt{C}}$.

If the system is now more generally described by an arbitrary superposition of $|L\rangle$ and $|R\rangle$, $|\Psi(t)\rangle = \alpha(t)|L\rangle + \beta(t)|R\rangle$, and if we choose the left-localized state $|L\rangle$ as the initial state of the SQUID, i.e., $|\Psi(t=0)\rangle = |L\rangle$, we obtain the time evolution

$$|\Psi(t)\rangle \propto |L\rangle \cos(\Delta Et/2) + i|R\rangle \sin(\Delta Et/2). \tag{6}$$

Thus, the wave function oscillates coherently between the two localized current states $|L\rangle$ and $|R\rangle$ in each well (see Fig. 2) at a rate determined by ΔE , since the probability to find the wave function localized in, say, the left well is oscillatory in time

$$P_L(t) = |\langle L|\Psi(t)\rangle|^2 = \cos^2(\Delta Et/2). \tag{7}$$

This leads to coherent quantum tunneling between the two wells and manifests itself in an oscillation of the current in the SQUID between clockwise and counterclockwise direc-

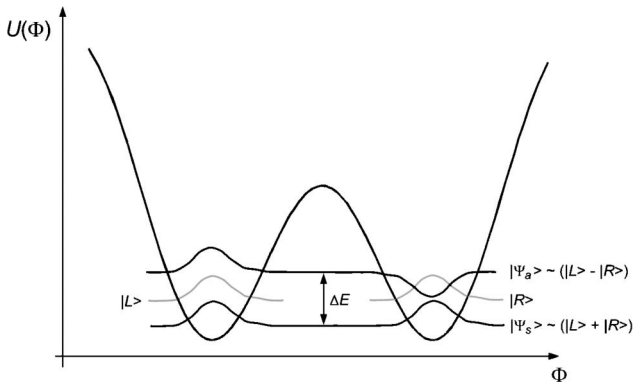


Fig. 1. Effective SQUID potential at bias $\Phi_{\text{ext}} = \Phi_0/2$. At this point, the double-well potential becomes symmetric. The degeneracy between the two fluxoid states $|L\rangle$ and $|R\rangle$ (which are localized in the left and right well of the potential and correspond to macroscopic currents running in opposite direction around the loop) is lifted by the formation of delocalized coherent superpositions $|\Psi_s\rangle = \frac{1}{\sqrt{2}}(|L\rangle + |R\rangle)$ (the symmetric ground state) and $|\Psi_a\rangle = \frac{1}{\sqrt{2}}(|L\rangle - |R\rangle)$ (the antisymmetric first excited state). The energy difference ΔE between $|\Psi_s\rangle$ and $|\Psi_a\rangle$ has been experimentally measured [38,37], which confirms the existence of superpositions of the macroscopically distinct states $|L\rangle$ and $|R\rangle$.



Fig. 2. Time evolution of the Wigner function corresponding to a superposition $|\Psi(t)\rangle \propto |L\rangle \cos(\Delta Et/2) + i|R\rangle \sin(\Delta Et/2)$ of the two localized opposite-current states $|L\rangle$ and $|R\rangle$ in a SQUID. The state coherently oscillates between the two wells, leading to coherent quantum tunneling. This manifests itself in a macroscopic current oscillating between clockwise and counterclockwise directions. Figure reprinted with permission from [39]. Copyright 2004 by the American Physical Society.

tions. This tunneling effect has been directly observed in superconducting qubit setups similar to the one described here [25,40–45].

The indirect route for detecting the presence of superpositions of states corresponding to macroscopic currents running in opposite directions relies on a static spectroscopic measurement of the energy difference ΔE (see Fig. 1). Friedman et al. [38] have confirmed the existence of such an energy gap (in excellent agreement with theoretical predictions) and, therefore, of superpositions of macroscopically distinct fluxoid states (see also [37] for a similar experiment and result). In their setup, $|L\rangle$ and $|R\rangle$ (which in this experiment corresponded to $k = 4$ and $k = 10$, respectively) differed in flux by more than $\Phi_0/4$ and in current by $2\text{--}3 \mu\text{A}$, corresponding to about $10^{10} \mu_B$ in local magnetic moment. Furthermore, the dynamics of the in-unison motion of the approximately 10^9 Cooper pairs represented by $|L\rangle$ and $|R\rangle$ are given by a single unitarily evolving wave function representing the collective flux coordinate Φ .

2.2.2. Scaling

A main advantage of SQUIDs over other experiments (such as those described in the subsequent sections) that probe the limits of quantum mechanics lies in the fact that the relevant macroscopic variable, namely, the trapped flux through the SQUID ring, can be controlled by means of microscopic energy differences in the Josephson junction [32]. As mentioned before, the tunneling matrix element scales as $e^{-\sqrt{C}}$, where C is dominantly determined by the junction rather than by the size of the loop. Thus the difficulty of observing superpositions of macroscopically distinct states scales essentially independently of the degree of macroscopic distinctness between these states (i.e., difference in flux between the opposite currents). This is in stark contrast to the matter-wave diffraction experiments and Bose–Einstein condensates discussed below. In the first case, the grating spacing must decrease as $1/\sqrt{N}$ with the number N of atoms in the molecule, in the second case the decoherence rate increases as N^2 with the number N of atoms in the condensate.

This particular property of SQUIDs has allowed for the creation of superpositions of states that differ by several orders of magnitude more than in other experiments (see Section 2.5).

2.2.3. The interpretation of superpositions

It is well known that quantum-mechanical superpositions must not be interpreted as a simple superposition (addition) of probability distributions. Formally, this conclusion is of course well reflected in the fact that, in quantum mechanics, we deal with superpositions of probability amplitudes rather than of probabilities, leading to interference terms in the probability distribution.

However, this crucial difference between classical and quantum-mechanical superpositions is sometimes not sufficiently clearly brought out when describing particular experimental situations. In the case of the standard double-slit interference experiment, for example, the state of the diffracted particle is described by a coherent superposition $|\psi\rangle = (|\psi_1\rangle + |\psi_2\rangle)/\sqrt{2}$ of the states $|\psi_1\rangle$ and $|\psi_2\rangle$ corresponding to passage through slits 1 and 2, respectively. This is frequently interpreted as simply representing simultaneous passage of the particle through both slits, i.e., presence of the particle in two distinct spatial regions at the same time, thereby tacitly neglecting the interference terms in the probability distribution.

In the double-slit example, this view will not necessarily be disproven until the stage of the screen is reached at which interference fringes appear. Similarly, and even more drastically, the superpositions of macroscopically distinct current states in a SQUID show that the simplified view of a classical superposition of probability distributions is inadequate. For, if this view were correct, the two contributing opposite currents would mutually cancel out and thus the net “current” described by this superposition would have to be zero, contrary to what is observed. Instead, the SQUID opposite-current superposition represents a novel individually existing physical state that can be described as a coherent “interaction” between simultaneously present states representing currents of opposite direction.

The SQUID example also shows that the “splitting” often referred to in an Everettian framework (for example, in DeWitt’s popularization of the “many-worlds view” [9–11]) should not be taken too literally. The transition, i.e., the “split,” from a single “classical” state—i.e., classically defined definite structures such as particles (defined as having a definite position), currents (defined as a flow of charge into a definite direction), etc.—into a state describing a superposition of such states occurs in a completely unitary and thus reversible manner by changing Φ_{ext} . There is only one single global state vector $|\Psi(t)\rangle$ at all times that corresponds to “physical reality.” The decomposition into a superposition of other states is a primarily formal procedure useful in revealing the physical quantities of our experience contained in the arbitrary state vector $|\Psi(t)\rangle$, since the latter can in general not be related to any “classical” physical structure that would correspond to directly observed objects or properties. In this sense, the “split” is simply a consequence of trying to trace throughout time a particular (usually “classical”) state that does not coincide with $|\Psi(t)\rangle$. Quantum mechanics shows that this can, in general, only be done in a relative-state sense.

The decomposition obtains also *physical* meaning when the dynamical evolution of the system described by $|\Psi(t)\rangle$ is considered, as the coefficients multiplying the “classical” terms in the superposition will in general be time-dependent. In the example of the SQUID, the coherent-tunneling state does not directly relate to a current in the classical sense (i.e., a current of definite direction), but it can be decomposed into two such currents of opposite direction. The physical relevance of this decomposition and the meaning of the superposition then manifests itself as a current that oscillates between clockwise and counterclockwise directions.

2.2.4. *Decoherence and the preferred basis*

A particularly interesting feature of the macrocurrent superpositions in SQUIDs is the fact that the interaction with the environment leads to a localization in flux space, rather than to the much more familiar and common localization in position space. In other words, the “preferred basis” (Zurek’s “pointer states” [4,46]) of the SQUID are flux eigenstates.

This observation is perfectly well accounted for by decoherence theory, which describes the selection of the preferred basis by means of the stability criterion, first formulated by Zurek [4] (see also [46,47,14,5,7]). According to this criterion, the basis used to represent the possible states of the system must allow for the formation of dynamically stable system–environment correlations. A sufficient (albeit not necessary) requirement for this criterion to be fulfilled is given by the condition that all basis projectors $\hat{P}_n = |s_n\rangle\langle s_n|$ of the system must (at least approximately) commute with the system–environment interaction Hamiltonian \hat{H}_{int} , i.e.,

$$[\hat{H}_{\text{int}}, \hat{P}_n] = 0 \quad \text{for all } n. \tag{8}$$

That is, the preferred basis of the system is given by a set of eigenvectors of \hat{H}_{int} .

In the case of the SQUID experiments at bias $\Phi_{\text{ext}} = \Phi_0/2$, if the interaction with the environment is very weak and thus the dynamics of the SQUID system are dominantly governed by the effective SQUID Hamiltonian \hat{H} , Eq. (3), the preferred states are predicted to be eigenstates of this Hamiltonian, namely, the delocalized coherent superpositions $|\Psi_s\rangle = \frac{1}{\sqrt{2}}(|L\rangle + |R\rangle)$ and $|\Psi_a\rangle = \frac{1}{\sqrt{2}}(|L\rangle - |R\rangle)$ of the localized zero-fluxoid and one-fluxoid states $|L\rangle$ and $|R\rangle$. This is in agreement both with the observation of coherent quantum tunneling between the wells and with the measurement of the energy gap $\Delta E = E_a - E_s$ between the states $|\Psi_s\rangle$ and $|\Psi_a\rangle$.

Under realistic circumstances, however, the SQUID is coupled to a dissipative environment \mathcal{E} which can quite generally be modeled as a harmonic heat bath of bosons [35], i.e., as a bath of N harmonic oscillators with generalized coordinates x_α and p_α , natural frequency ω_α , mass m_α , and Hamiltonian

$$\hat{H}_{\mathcal{E}} = \frac{1}{2} \sum_{\alpha=1}^N \left(\frac{p_\alpha^2}{m_\alpha} + m_\alpha \omega_\alpha^2 x_\alpha^2 \right). \tag{9}$$

The reservoir modes x_α couple dynamically to the total flux variable Φ of the SQUID ring. More precisely, they couple to the fluxoid (and essentially opposite-current) states $|L\rangle$ and $|R\rangle$ via the interaction Hamiltonian [35]

$$\hat{H}_{\text{int}} = -\sigma_z \left(\frac{\varphi_0}{2} \sum_{\alpha} c_\alpha x_\alpha \right), \tag{10}$$

where $\sigma_z = (|L\rangle\langle L| - |R\rangle\langle R|)$ is the so-called “pseudospin” operator (owing its name to the fact that the SQUID double-well system can be effectively mapped onto a two-state spin system, with $|L\rangle$ and $|R\rangle$ corresponding to, say, spin “up” and “down,” respectively), and $\pm\varphi_0$ are the flux values associated with the two localized states $|L\rangle$ and $|R\rangle$.

According to the commutativity criterion, Eq. (8), the stable states into which the system decoheres are then eigenstates of σ_z , i.e., the preferred basis of the system is given by the two states $|L\rangle$ and $|R\rangle$. This, of course, is in full agreement with observations and explains the localization in flux space, i.e., the rapid reduction of the superposition into an apparent ensemble of the macroscopically distinguishable current states $|L\rangle$ and $|R\rangle$.

Fig. 3 illustrates this gradual disappearance of interference in the symmetric ground state $|\Psi_s\rangle = \frac{1}{\sqrt{2}}(|L\rangle + |R\rangle)$ due to the interaction of the SQUID ring with a dissipative thermal bath in the Wigner representation of the local density operator of the SQUID [39] (see also [48]). As predicted by the stability criterion, the robust states (i.e., the preferred basis) selected by the environment are the macroscopically distinguishable current states $|L\rangle$ and

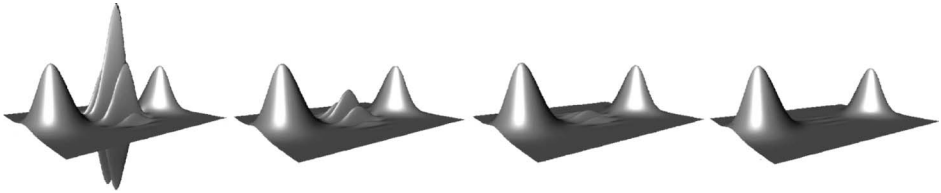


Fig. 3. Decoherence of the symmetric ground state $|\Psi_s\rangle = \frac{1}{\sqrt{2}}(|L\rangle + |R\rangle)$ at bias $\Phi_{\text{ext}} = \Phi_0/2$ in the Wigner representation. The interaction of the SQUID loop with the environment (here modeled as a monochromatic thermal bath) locally destroys the interference between the two “classical” flux states $|L\rangle$ and $|R\rangle$ represented by the localized peaks on either side. Figure reprinted with permission from [39]. Copyright 2004 by the American Physical Society.

$|R\rangle$. The resulting local loss of coherence—that is, the distribution of coherence, initially associated with the SQUID, over the many degrees of freedom of the SQUID-environment combination—constitutes the main obstacle in the observation of coherent quantum tunneling.

2.3. Molecular matter-wave interferometry

Recent experiments by the group of Zeilinger co-workers [49–57] have pushed the boundary for the observation of quantum (“wave”) behavior towards larger and larger particles. In the experiment to be described, mesoscopic C_{60} molecules (so-called fullerenes) and C_{70} molecules have been observed to lead to an interference pattern following passage through a diffraction grating (“matter-wave interferometry”). The carbon atoms in the C_{70} molecule are arranged in the shape of an elongated buckyball with a diameter of about 1 nm (see Fig. 4). They are complex and massive enough to exhibit properties that position them in the realm of classical solid objects rather than that of atoms. For example, they possess a large number of highly excited internal rotational and vibrational degrees of freedom that allow one to attribute a finite temperature to each individual molecule, and heated C_{70} molecules are observed to emit photons and electrons. The particle aspect seems to be overwhelmingly clear, and yet these molecules have been shown to exhibit quantum interference effects.

2.3.1. Experimental setup and observation of interference

The observation of C_{70} interference patterns and their controlled disappearance due to environmental decoherence induced by various sources has been made possible by the so-

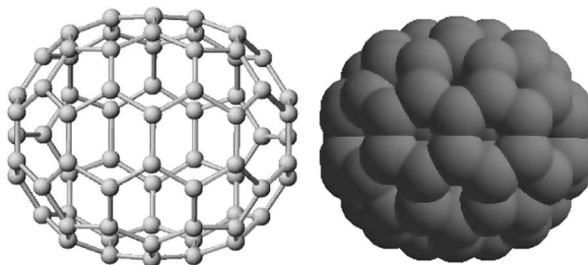


Fig. 4. Illustration of a C_{70} molecule. The left image shows the “backbone” structure of interlinked carbon atoms. The right image displays the carbon atoms as massive spheres.

called Talbot–Lau interferometer [50] that has two main advantages over earlier setups used for molecular interferometry [58,59]. First, the incident beam of molecules does not need to be collimated, allowing for much higher transmitted intensities. Second, the required period of the gratings used to obtain the interference pattern scales only with the square root of the de Broglie wavelength of the molecules, allowing for the probing of the quantum behavior of, say, 16 times larger molecules by using an only four times smaller grating spacing.

The Talbot–Lau effect is based on the fact that the transverse part of a plane wave $\psi(z) = e^{ikz}$ incident on a periodic grating located in the xy plane will be identical to the grating pattern at integer multiples of the distance (“Talbot length”)

$$L_\lambda = \frac{d^2}{\lambda} \quad (11)$$

behind the grating. Since this is a pure interference effect, the presence of the grating pattern at multiples of the Talbot length indicates the wave nature of the incident beam.

The experimental setup that makes use of the Talbot–Lau effect is shown schematically in Fig. 5. The main part consists of a set of three gold gratings with a period of about $d = 1 \mu\text{m}$. The first grating acts as a collimator that induces a sufficient degree of coherence in the incident uncollimated beam of C_{70} molecules to approximate the plane-wave assumption made above. Each point of the grating can then be viewed as representing a narrow source. The velocity of the molecules can be selected over a range from about 80 to 220 m/s, corresponding to de Broglie wavelengths of approximately 2–6 pm. The second grating is the actual diffraction element, assuming the role of the single grating in the above plane-wave example. The third grating, placed behind the second grating at a distance L equal to the Talbot length $L_{\lambda_{C_{70}}} = d^2/\lambda_{C_{70}}$, where $\lambda_{C_{70}}$ is the de Broglie wavelength of the molecules, can be moved in the x -direction and serves as a scanning detection mask for the molecular density pattern in the transverse plane at this location. The molecules that have passed through the third grating are ionized by a laser beam and then counted by an ion detector.

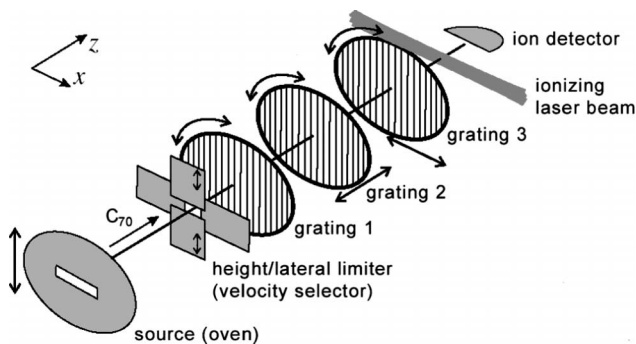


Fig. 5. Schematic sketch of a Talbot–Lau interferometer used for demonstrating quantum behavior of mesoscopic C_{70} molecules. The first grating induces a certain degree of coherence in the incident uncollimated beam of molecules. The second grating then acts as the actual diffraction stage. Due to the Talbot–Lau effect, the molecular density pattern at the position of the third grating will be an image of the second grating if the molecules possess a quantum-wave nature. Scanning this pattern by moving the third grating (which acts as a mask) in the x -direction and detecting the transmitted and subsequently ionized molecules will then lead to an oscillatory signal that represents the interference effect. Figure reprinted with permission from [50]. Copyright 2002 by the American Physical Society.

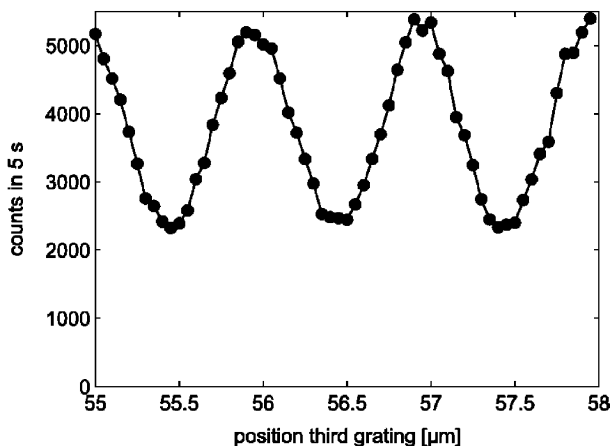


Fig. 6. Interference fringes for C_{70} molecules measured at the position of the third grating in a Talbot–Lau interferometer. Figure reprinted with permission from [50]. Copyright 2002 by the American Physical Society.

If the C_{70} molecules indeed possess a quantum-wave nature, the Talbot–Lau effect implies that the molecular density pattern at the position of the third grating should consist of interference fringes with a period equal to the spacing d of the grating pattern. Thus, when the third grating is scanned in the x -direction, we expect an oscillation in the number of transmitted molecules with period d . This is indeed what has been observed experimentally [49,52,50,53,54] (Fig. 6). The possibility that these fringes could result from a classical blocking of rays by the gratings (Moiré fringes) can be excluded, because such patterns would be independent of the de Broglie wavelength, in contrast to what is observed experimentally [50,55]. This confirms the quantum origin of the measured fringes and thus the wave nature of the C_{70} molecules.

It should be emphasized that the fringes represent *single-particle* interference effects, rather than being due to interference between different molecules [53]. The latter case would require the interfering molecules to be in the same state, which is practically never the case due to the large number of different excited internal states. Furthermore, the density in the molecular beam is relatively low, such that the average distance between two molecules is much greater than the range of any intermolecular force. Thus, even if the molecules passed at such a slow rate through the apparatus that only a single molecule was present at any time, an interference pattern would emerge. The interference effect is entirely due to the splitting and overlapping of the wave fronts associated with each individual C_{70} molecule. This demonstrates clearly that quantum-mechanical superpositions in configuration space describe individual states that can exhibit interference effects (i.e., phase dependencies) without any statistical aspect.

2.3.2. Disappearance of interference due to controlled decoherence

General numerical estimates for decoherence rates derived from theoretical expressions [60–63] have clearly demonstrated the extreme efficiency of decoherence on mesoscopic and macroscopic scales. It is therefore usually practically impossible to control the environment in such a way as to explicitly resolve and observe the gradual action of decoherence on larger objects.

The Talbot–Lau interferometer, however, has made such observations possible and has also led to direct confirmations of the predictions of decoherence theory for mesoscopic objects [55,54,56,64,57]. The main sources of decoherence that have been experimentally investigated are collisions with gas molecules present in the interferometer [54,55,64], and thermal emission of radiation when the C_{70} molecules are heated to temperatures beyond 1000 K [56,57]. Here, we shall focus on the first case of decoherence, as collisions with environmental particles represent the most natural and ubiquitous source of decoherence in nature.

In the experiments, the vacuum chamber containing the interferometer is filled with gases at different pressures. Each collision between a gas particle and a C_{70} molecule entangles their motional states. Since the C_{70} molecules are much more massive than the gas molecules, the motional state of the gas molecule is distinguishably changed in the collision, while the motion of the C_{70} molecule remains essentially unaffected and can therefore still be detected at the third grating. Thus, each collision encodes which-path information about the trajectory of the C_{70} molecule in the environment (i.e., in the colliding gas particle). This leads to decoherence in the spatial wave function of the C_{70} molecules, since the post-collision environmental states are approximately orthogonal in the position basis due to the significant change of the motional state of the gas molecules in the collisions.

To see this more explicitly, let us denote the state of the C_{70} molecule before and after the scattering by

$$|\psi\rangle_{C_{70}} = \int d\mathbf{x} (\langle \mathbf{x} | \psi \rangle)_{C_{70}} |\mathbf{x}\rangle_{C_{70}} \quad (12)$$

and

$$|\psi'\rangle_{C_{70}} = \int d\mathbf{x} (\langle \mathbf{x} | \psi' \rangle)_{C_{70}} |\mathbf{x}\rangle_{C_{70}}, \quad (13)$$

respectively, where

$$(\langle \mathbf{x} | \psi \rangle)_{C_{70}} \approx (\langle \mathbf{x} | \psi' \rangle)_{C_{70}} \quad (14)$$

for all \mathbf{x} . A collision at \mathbf{X} changes the state of the colliding gas molecule from $|\varphi\rangle_{\text{gas}}$ to $|\varphi', \mathbf{X}\rangle_{\text{gas}}$, which encodes which-path information about the C_{70} molecule. Since the $|\varphi', \mathbf{X}\rangle_{\text{gas}}$ represent distinguishable motional states, the environmental states corresponding to scattering events at different locations become approximately orthogonal

$$(\langle \varphi', \mathbf{X} | \varphi', \mathbf{Y} \rangle)_{\text{gas}} \approx \delta(\mathbf{X} - \mathbf{Y}). \quad (15)$$

The collision leads to an entangled state for the combined gas– C_{70} system

$$|\Psi_0\rangle = |\psi\rangle_{C_{70}} \otimes |\varphi\rangle_{\text{gas}} \rightarrow |\Psi\rangle \approx \int d\mathbf{X} (\langle \mathbf{X} | \psi \rangle)_{C_{70}} |\mathbf{X}\rangle_{C_{70}} \otimes |\varphi', \mathbf{X}\rangle_{\text{gas}}. \quad (16)$$

The reduced density matrix for the C_{70} molecule expressed in the position basis is then obtained by averaging over all possible states $|\varphi', \mathbf{X}\rangle_{\text{gas}}$ of the gas molecule

$$\begin{aligned} \rho_{C_{70}} &\approx \int d\mathbf{X} \int d\mathbf{X}' \int d\mathbf{X}'' (\langle \mathbf{X} | \psi \rangle)_{C_{70}} (\langle \mathbf{X}' | \psi \rangle)_{C_{70}}^* (\langle \varphi', \mathbf{X}'' | \varphi', \mathbf{X} \rangle)_{\text{gas}} \\ &\quad \times (\langle \varphi', \mathbf{X}' | \varphi', \mathbf{X}'' \rangle)_{\text{gas}} (|\mathbf{X}\rangle \langle \mathbf{X}'|)_{C_{70}} \\ &\approx \int d\mathbf{X} |(\langle \mathbf{X} | \psi \rangle)_{C_{70}}|^2 (|\mathbf{X}\rangle \langle \mathbf{X}|)_{C_{70}}, \end{aligned} \quad (17)$$

where the vanishing of interference terms $(\langle \mathbf{X} | \psi \rangle)_{C_{70}} (\langle \mathbf{X}' | \psi \rangle)_{C_{70}}^*$, $\mathbf{X} \neq \mathbf{X}'$, in the last step follows from the approximate orthogonality of the $|\varphi', \mathbf{X}\rangle_{\text{gas}}$. Thus, the gas molecules carry away which-path information, leading to a diffusion of coherence into the environment. Incidentally, in this sense, Bohr’s complementarity principle can be understood as a consequence of entanglement: The observability of an interference pattern, and thus the degree of the “wave aspect” of the C_{70} molecules, is directly related to the amount of information, encoded through entanglement with the state of the gas particles, about the path (the “particle aspect”) of the molecules.

We expect the visibility V_λ of the interference fringes (defined as $(c_{\text{max}} - c_{\text{min}})/(c_{\text{max}} + c_{\text{min}})$, where c_{max} and c_{min} are the maximum and minimum amplitudes of the interference pattern) to decrease as the pressure of the environmental gas is increased. A theoretical analysis [55,63,64] predicts that V_λ will decrease exponentially with the pressure $p = nk_B T$ of the colliding gas,

$$V_\lambda(p) = V_\lambda(0)e^{-p/p_0}. \tag{18}$$

Here,

$$p_0 = \frac{k_B T}{2L\sigma_{\text{eff}}} \tag{19}$$

is the characteristic decoherence constant (“decoherence pressure”), where L denotes the distance between the gratings and σ_{eff} corresponds to the effective cross section [55]. This pressure-dependent decay of the visibility has indeed been confirmed experimentally for C_{70} molecules [55,54], in excellent agreement with the theoretical predictions (Fig. 7).

Studies of collision-induced decoherence in a Talbot–Lau interferometer not only represent an outstanding method to observe the gradual disappearance of quantum-interference effects while having full control over both the source and the strength of decoherence, but also allow one to predict the environmental conditions (in this case, the maximum pressure of the surrounding gas) required to observe quantum effects for even more complex and massive objects than tested thus far. Such experiments are limited by two main factors [54,55]. First, the velocity of the objects must be quite slow during the passage

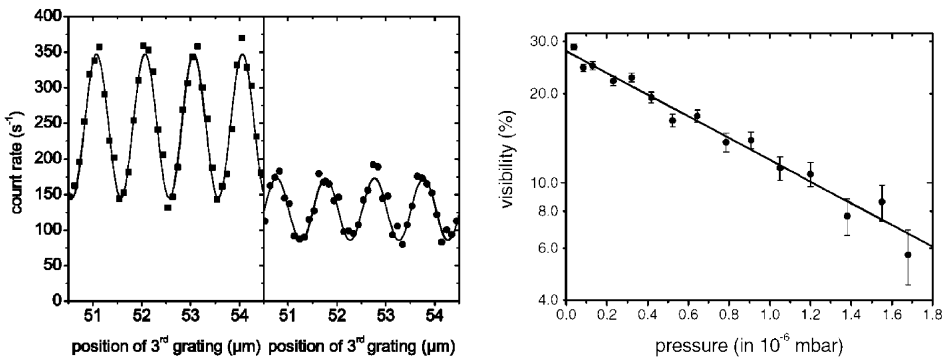


Fig. 7. Diminished interference effect in C_{70} -molecule interferometry due to decoherence induced by collisions with gas molecules. Above: Decreased visibility of the interference fringes when the pressure of the gas is increased from the left to the right panel. Below: Dependence of the visibility on the gas pressure. The measured values (circles) are seen to agree well with predictions obtained from decoherence theory (solid line), see Eqs. (18) and (19). Figures reprinted, with kind permission of Springer Science and Business Media, from [55].

through the interferometer, to keep the de Broglie wavelengths long enough to allow for a sufficient degree of diffraction by practically realizable gratings. Second, the pressure p of the residual gas in the interferometer must be low enough to maintain sufficient visibility of the interference pattern, i.e., we must have $O(p) = p_0$, see Eq. (19). Since both limits are purely technical and can be precisely quantified, there is no indication for any fixed quantum-classical boundary in this case other than the observational limit determined by environmental decoherence, for which rigorous theoretical estimates can be given. Decoherence allows for an exact specification of where the quantum-to-classical transition occurs and what needs to be done to move the boundary.

In fact, the envelope for the observation of the wave nature of mesoscopic molecules has recently been pushed even further in experiments demonstrating quantum interference fringes for the important biomolecule tetraphenylporphyrin $C_{44}H_{30}N_4$ (with mass $m = 614$ amu and a width over 2 nm) and for the fluorinated fullerene $C_{60}F_{48}$ (mass $m = 1632$ amu, 108 atoms) Fig. 8 [51]. While tetraphenylporphyrin is the first-ever biomolecule whose

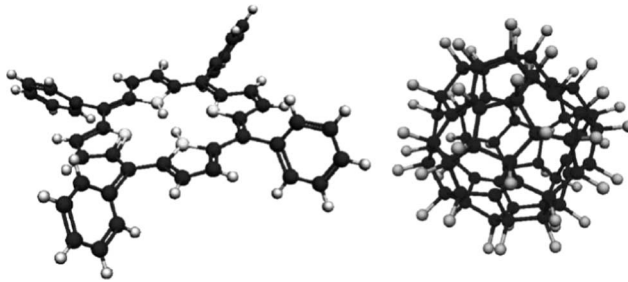


Fig. 8. Structure of the biomolecule tetraphenylporphyrin $C_{44}H_{30}N_4$ (left) and of the fluorofullerene $C_{60}F_{48}$ (right). The wave nature of both molecules has been observed in experiments. Figures reprinted with permission from [51]. Copyright 2003 by the American Physical Society.

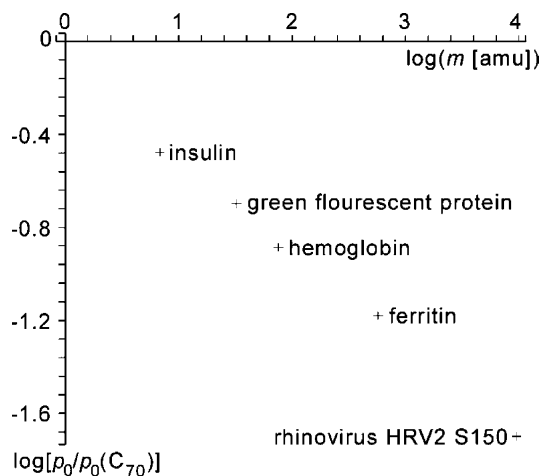


Fig. 9. Extrapolated maximum residual air pressures p_0 , relative to the value of p_0 for C_{70} molecules, versus molecular weight m (in amu), that would allow for an observation of interference fringes for various biological structures in an elongated ($L = 1$ m) Talbot–Lau interferometer. Data from [55].

wave nature has been demonstrated experimentally, fluorofullerenes are the most massive and complex molecules to exhibit quantum behavior thus far. Theoretical estimates for the maximum residual gas pressure that would still allow for the observation of interference fringes for even larger biological objects, up to the size of a rhinovirus, have been given by Hackermüller et al. [52,55] (see Fig. 9) and appear to be realizable even with the currently available technology in Talbot–Lau interferometry [54,55]. One might extrapolate even further and speculate about the feasibility of interference experiments involving human cells, with an average weight and size on the order of 10^{15} amu and 10^4 nm, respectively. While this is certainly beyond the existing technology, there is no reason to assume that such experiments should be impossible.

2.3.3. Implications of the C_{70} interference experiments

The described matter-wave interferometry experiments have led to three crucial results:

- (1) Interference patterns are observed for particles that clearly reside in the “lump of matter” category.
- (2) These patterns are due to single-particle (rather than interparticle) interference effects.
- (3) Any observed disappearance (or absence) of interference patterns can be well understood as resulting from decoherence and can be explicitly controlled and quantified.

Thus there is no theoretical or experimental indication for any fundamental limit on the ability of objects to exhibit quantum behavior (i.e., a wave nature) if these objects are sufficiently shielded from the decohering influence of their environment. Result (2) shows that the initial wave function describing the individual molecule evolves into a spatially extended wave function after passage through the diffraction grating, namely, into a superposition of “classical” localized position states that each correspond to the molecule being in a specific region of space. The gradual disappearance of interference due to controlled interaction with the environment can be understood as entanglement between the different relative states of the environment and the individual components $|\mathbf{x}\rangle_{C_{70}}$ in the superposition. It is important to note that all components $|\mathbf{x}\rangle_{C_{70}}$ are still present regardless of the environmental interaction—decoherence is in principle fully reversible, as experiments on coherent state-vector revival have shown (see, e.g., [31]).

2.4. Bose–Einstein condensation

As a third example, we shall discuss Bose–Einstein condensation (BEC). While this effect had been predicted theoretically already in the 1920s by Einstein [67–69] based on ideas by Bose [70], explicit experimental verification succeeded only in 1995 [71–74]. When an atomic bosonic gas confined by a magnetic trap is cooled down to very low temperatures, the de Broglie wavelength $\lambda_{dB} = (2\pi\hbar^2/mk_B T)^{1/2}$ associated with each atom becomes long in comparison with the interparticle separation. At a precise temperature in the ≈ 100 nK range, the collection of atoms can undergo a quantum-mechanical phase transition to a condensate in which the atoms lose their individuality and all occupy the same quantum state. Then a macroscopic number of atoms—large condensates can contain of the order of 10^7 atoms—is described by a single N -particle wave function with a phase,

$$\Psi_N(\mathbf{r}_1, \mathbf{r}_1, \dots, \mathbf{r}_N) = e^{i\phi} \prod_{i=1}^N |\psi(\mathbf{r}_i)|, \quad (20)$$

i.e., as a product of N identical single-particle wave functions $\psi(\mathbf{r})$. As a consequence, BECs can directly exhibit quantum behavior. For instance, two condensates released from adjacent traps can overlap and form a gas-density interference pattern due to the phase difference between the two wave functions (Fig. 10) [75,65,76–78]. Recently, Bose–Einstein “double-slit” interferometers have been experimentally realized [66] and theoretically analyzed [79]. Here, a single condensate is coherently split (corresponding to the diffraction stage in the double-slit experiment) and then allowed to recombine, which leads to the observation of interference fringes (Fig. 10).

2.4.1. Macroscopic number-difference superpositions using Bose–Einstein condensates

Various methods have been proposed for the creation of BEC-based Schrödinger cat states in form of a superposition of states with macroscopically distinguishable numbers of particles [80–86]. BECs are particularly suitable for the generation and the study of Schrödinger cat states, for several reasons. First, as BECs involve up to 10^7 atoms, such superpositions would be the most macroscopic ones ever observed. Second, the condensate is described by a single coherent wave function that pertains to a controllable number of atoms and possesses an extremely long coherence time (up to 10–20 s). Third, the sources of decoherence (mostly loss of particles from the condensate) are fairly well-understood and potentially sufficiently controllable through suitable environmental engineering and trap design [87–89].

The typically suggested scheme to create superpositions of macroscopically distinguishable states using BECs involves the creation and manipulation of interacting two-species condensates, i.e., BECs in which the atoms possess two different internal states $|A\rangle$ and $|B\rangle$. Experimental realizations of two-species BECs often employ the two hyperfine sublevels $|F, m_F\rangle = |2, 1\rangle$ and $|1, -1\rangle$ of ^{87}Rb . The early proposal by Cirac et al. [80] (similar models have been suggested, for example, in [81–83,86,90]) is based on a Josephson-like coupling between the two species that leads to a number-difference superposition of the form

$$|\Psi\rangle = \frac{1}{\sqrt{2}}(|n_A, N - n_A\rangle + e^{i\phi}|N - n_A, n_A\rangle), \quad (21)$$

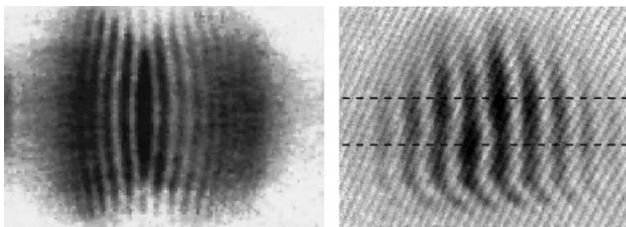


Fig. 10. Matter-wave interference pattern for the atomic gas density in Bose–Einstein condensates. (Left) Pattern obtained by letting two independent condensates overlap, demonstrating that the condensate is indeed described by a single wave function with a phase. The fringe period was measured to be $20 \mu\text{m}$. Figure reprinted with permission [65]. Copyright 1997 by AAAS. (Right) Fringes due to interference of a single coherently split condensate. This experiment corresponds to a BEC “double-slit” interferometer. Figure reprinted with permission from [66]. Copyright 2004 by the American Physical Society.

where $|n_A, n_B\rangle$ is the occupation-number state representing n_A atoms of type A and n_B atoms of type B, and $N = n_A + n_B$ is the total number of atoms. This represents a superposition of two states which differ by a macroscopic number $|N - 2n_A|$ of atoms of a certain type (A or B). Then $n_A = 0$ or $n_A = N$ would correspond to a maximally entangled N -particle GHZ-type state [33] and thus the most “cat-like” state

$$|\Psi\rangle = \frac{1}{\sqrt{2}}(|N, 0\rangle + e^{i\varphi}|0, N\rangle). \quad (22)$$

Another scheme for the creation of macroscopic BEC superpositions that uses a single-component BEC in a double well (with possible generalizations to M wells) has been described in [91,92] (see also [93,94]). Here, a laser-induced phase shift is imprinted on the condensate in one of the wells, followed by a change of barrier height. This is predicted to lead to a superposition of the form

$$|\Psi\rangle = \frac{1}{\sqrt{2}}(|n_L, N - n_L\rangle + e^{i\varphi}|N - n_L, n_L\rangle), \quad (23)$$

where $|n_L, n_R\rangle$ is the number state corresponding to n_L (n_R) atoms in the left (right) well. Again, n_L determines the degree of entanglement, with $n_L = 0$ or $n_L = N$ corresponding to maximal “catness.” Even the possibility of creating a coherent superposition of a macroscopic number of atoms with a macroscopic number of molecules using photoassociation in BECs (i.e., the absorption of a photon by two atoms, leading to the formation of a two-atomic bound molecule) has been indicated [84].

To detect a BEC cat state, one might in principle envision experiments similar to those measuring GHZ spin states [95,89,96], although this would be very difficult to carry out in practice for the larger values of N relevant to BEC superpositions. Instead, as pointed out in [89], one could first confirm that measurement statistics indeed give equal likelihoods for the two cat-state terms $|N, 0\rangle$ or $|0, N\rangle$. If the system can also be observed to (approximately) return to its initial state after unitary evolution over a period that is an integer multiple of the time needed for the generation of the cat state, this would provide strong indications for the presence of a cat state.

2.4.2. Decoherence of BEC superpositions

To date, Schrödinger-cat states using BECs have not been realized experimentally, although much progress has been made (see, for example, [97]). Dissipation and decoherence effects are still too strong to allow for a direct observation of superpositions and will continue to constitute the dominant limit on the size of number-difference Schrödinger cats. These environmental effects are mainly due to elastic and inelastic scattering between condensate and noncondensate atoms.

Elastic collisions with noncondensate atoms under conservation of the number of condensate atoms lead to phase damping and thus to the destruction of the coherent superposition. The reduced density matrix in the number basis then decoheres according to [85]

$$\langle m|\hat{\rho}(t)|n\rangle = e^{-(m-n)^2\kappa t} \langle m|\hat{\rho}(0)|n\rangle e^{-i\omega(m-n)t}, \quad (24)$$

i.e., the off-diagonal elements $m \neq n$ decay with a decoherence rate that scales with the square of the number difference, $(m - n)^2$.

Furthermore, inelastic collisions with noncondensate atoms lead to a loss of atoms from the condensate, which diminishes coherence. Again, the larger the number difference in the superposition $(|n, N-n\rangle + |N-n, n\rangle)/\sqrt{2}$ is (i.e., the closer n is to 0 or N), the more sensitive the state is to atom loss (see, for example, the detailed analysis in [83]). In the limit of the maximally entangled state $(|N, 0\rangle + |0, N\rangle)/\sqrt{2}$, already the loss of a single atom of, say, type 1 completely destroys the coherent superposition, since

$$\hat{a}_1(|N, 0\rangle + e^{i\varphi}|0, N\rangle)/\sqrt{2} = \sqrt{N/2}|N-1, 0\rangle, \quad (25)$$

where \hat{a}_1 is the destruction operator for particles of type 1.

Thus both decoherence effects will usually limit the size N (i.e., the number difference) of superpositions of the form $(|N, 0\rangle + |0, N\rangle)/\sqrt{2}$. In a detailed analysis that combines the two forms of scattering processes, Dalvit et al. [89] have estimated the decoherence rate τ_d^{-1} for an optimal number-difference superposition $(|N, 0\rangle + |0, N\rangle)/\sqrt{2}$ in a standard harmonic trap due to a “thermal cloud” of N_{nc} noncondensate atoms as

$$\tau_d^{-1} \propto a^2 N_{nc} N^2, \quad (26)$$

where a is the scattering length. This leads to very short decoherence times even for moderate environment and condensate sizes [89,85]. For example, for $N_{nc} = 10$ and $N = 10^3$, τ_d is of the order of milliseconds. For larger Schrödinger cats with $N = 10^7$ and a thermal cloud containing $N = 10^4$ noncondensed atoms, $\tau_d \sim 10^{-13}$ s.

However, several schemes exist to significantly reduce the decoherence rate and to thus render it quite likely that BEC-based number-difference Schrödinger cat states could indeed be observed in future experiments; for example:

- (1) The construction of modified traps that allow for a faster evaporation of the thermal cloud [89].
- (2) Generation of number-difference cat states via the creation of macroscopic superpositions of relative-phase states that are not only much less sensitive to atom loss, but might even *require* such loss [83].
- (3) A “symmetrization” of the environment to reduce the effective size of the thermal cloud [89].
- (4) Sufficiently fast generation of the cat state [86].

The key lesson to be learned from the example of BEC-based Schrödinger-cat states is that, notwithstanding the fact that such superpositions have not (yet) been explicitly documented in experiments, the physics of these states and the required conditions to create them is very well understood. The failure to experimentally generate these states with currently available setups is well-explained by decoherence models that provide precise numerical estimates for the type of experimental arrangements and parameter ranges that would be required to observe Schrödinger-cat states using BECs. Similar to the case of studying the feasibility of matter-wave interferometry with larger molecules than those investigated thus far (see Section 2.3), decoherence is the key tool for a precise prediction of the physical conditions required for the experimental observation of superpositions of macroscopically distinct states.

2.5. Analysis of the degree of macroscopicity of the experimentally achieved superpositions

In the following, let us compare the degree of macroscopic distinctness of the states in the superpositions encountered in the experiments with SQUIDs, diffracted molecules, and BECs. We will use the combination of the two measures introduced in Section 2.1, namely, the difference \mathcal{S}_{ext} in a relevant extensive quantity between the states in the superposition relative to an appropriate microscopic reference value, and the degree of entanglement \mathcal{S}_{ent} present in the multi-particle superposition.

For the SQUID experiments (Section 2.2), choosing the total magnetic moment to be the relevant extensive variable, the two states $|L\rangle$ and $|R\rangle$ differ by about $10^{10}\mu_{\text{B}}$ in the experiment by Friedman et al. [38]. Taking the Bohr magneton μ_{B} as the reference unit, the extensive difference \mathcal{S}_{ext} between the two states is thus of the order of 10^{10} . The degree of entanglement \mathcal{S}_{ent} in the multi-Cooper-pair state can be estimated to be of the order of the number of Cooper pairs, i.e., $\sim 10^9$.

In the case of diffraction of C_{70} molecules (Section 2.3), a suitable extensive quantity would be the center-of-mass displacement between the two paths through the interferometer, which we can estimate to be on the order of 1 mm (corresponding to the lateral width of the molecular beam [55]) relative to the size of the molecule of about 1 nm, which yields a value for \mathcal{S}_{ext} on the order of 10^6 . The degree of entanglement \mathcal{S}_{ent} is essentially given by the number of microscopic constituents in the molecule, $3 \times 6 \times 70 \sim 10^3$.

For BEC two-species superpositions that use the two hyperfine sublevels $|F, m_F\rangle = |2, 1\rangle$ and $|1, -1\rangle$ of ^{87}Rb atoms (Section 2.4), a suitable extensive variable would be the total difference in angular momentum due to the hyperfine splitting, in units of \hbar , which is on the order of the number N of atoms in the condensate, which can be as large as 10^7 . Thus the maximum \mathcal{S}_{ext} is on the order of 10^7 . The degree of entanglement \mathcal{S}_{ent} is again suitably measured by the number of nucleons and electrons in the condensate, which is of the order of $100N$ for ^{87}Rb . Note, however, that such superpositions have not yet been experimentally achieved.

All values are summarized in Table 1. We see that the SQUID experiments allow for superpositions that are about 10 orders of magnitude “more macroscopic” (in the sense defined above) than those achieved by molecular interferometry. On the other hand, the latter experiments lead to a direct realization of spatial superpositions, which are often considered to be more “counterintuitive” than the superposition of superconducting currents, since position appears to be the dominant definite quantity in our observation of the macroworld. The ubiquitous perception of definiteness in position space has even led some to postulate a fundamentally preferred role to position. For example, Bell [98] stated that “in physics the only observations we must consider are position observations, if only the positions of instrument pointers.” A similar idea underlies the spatial localization mechanism in the GRW theory and is reflected in the concept of definite particle trajectories in Bohmian mechanics.

Superpositions involving two-species BECs, if experimentally realized, would come close to the degree of macroscopicity achieved in SQUIDs. This result can be understood by noting the striking analogies between the two experiments. In both cases, the multi-particle system (the superconducting material in SQUIDs, or the atomic gas in BECs) is cooled down to extremely low temperatures near absolute zero. The two macroscopically distinguishable states (currents of opposite direction in SQUIDs, or different atom species

Table 1

Estimates for the degree of macroscopic distinctness of the states in superpositions relevant to the three experiments discussed in this paper

Experiment	\mathcal{S}_{ext}	\mathcal{S}_{ent}	$\mathcal{S}_{\text{ext}} \times \mathcal{S}_{\text{ent}}$
SQUID	10^{10}	10^9	10^{19}
C_{70}	10^6	10^3	10^9
Bose–Einstein ^a	10^7	10^9	10^{16}

\mathcal{S}_{ext} is a measure for the maximum difference in a suitably chosen extensive variable that distinguishes the states in the superposition (here: the total magnetic moment in SQUID experiments; the average separation between two paths in the interferometer in C_{70} molecular diffraction; the difference in angular momentum in two-species Bose–Einstein condensates). \mathcal{S}_{ent} measures the degree of entanglement in multi-particle states and is well-estimated by the number of microscopic constituents involved in the superposition (i.e., the number of Cooper pairs in SQUID, and the number of nucleons and electrons in the C_{70} molecule and the Bose–Einstein condensate). The third column shows the product $\mathcal{S}_{\text{ext}} \times \mathcal{S}_{\text{ent}}$ of the two measures, thus representing the overall degree of macroscopicity of the superpositions. See also Section 2.1.

^a Not yet experimentally achieved.

in BECs) are coupled by a classically impenetrable barrier of the Josephson-junction type. In both experiments, this essentially leads to Schrödinger-cat states of the form

$$|\Psi\rangle = \frac{1}{\sqrt{2}}(|N, 0\rangle + e^{i\varphi}|0, N\rangle), \quad (27)$$

where the number state $|N, 0\rangle$ denotes N particles (Cooper pairs in SQUIDS, or atoms in BECs) being in the first macroscopically distinguishable state (representing a clockwise current in the SQUID, or the hyperfine sublevel $|F, m_F\rangle = |2, 1\rangle$ in BECs), and no particles being in the second state (corresponding to a counterclockwise current in the SQUID, or the hyperfine sublevel $|F, m_F\rangle = |1, -1\rangle$ in BECs).

3. The status of physical collapse models

All existing interpretations of quantum mechanics can be viewed as either adding formal rules¹ or physical elements (as in collapse models) to the axioms of minimal quantum theory stated in Section 1. With respect to the “formal” category, if the minimal theory can be shown to be sufficient to explain and predict all our observations, there is clearly no empirical reason for introducing purely formal additives. While a similar argument can be made regarding the “physical” category, collapse theories might lead to observable deviations from Schrödinger dynamics and could thus be experimentally tested. In both cases, of course, there may be conceptual reasons that motivate the added elements, for example a desire to resolve a felt “weirdness” in the existing quantum theory. While we respect this motivation, we hope to show that in fact the minimal theory is sufficient to resolve the problems without requiring any such additions.

The increasing size of physical systems for which interference effects have been observed imposes bounds on the parameters used in collapse models. However, the current experiments demonstrating mesoscopic and macroscopic interference are still quite far away

¹ As, for example, done in the Copenhagen interpretation (that formally postulates a collapse, but regards it merely as an “increase of information,” rather than as a physical process, since it interprets the wave function as representing a probability amplitude), Bohmian mechanics, modal interpretations, and consistent-histories interpretations.

from disproving the existing collapse theories. For example, even the C_{70} diffraction experiments described in Section 2 still fall short of ruling out continuous spontaneous localization models [99–101] (which lead to the strongest deviations from Schrödinger dynamics among all physical collapse theories) by 11 orders of magnitude [102]. A recently proposed mirror-superposition experiment by Marshall et al. [103] that might lead to a superposition involving of the order of 10^{14} atoms still fails to rule out continuous spontaneous localization models by about 6 orders of magnitude [104]. The superpositions observed in coherent quantum tunneling in SQUIDs also appear to be compatible with dynamical reduction models, since the spatial localization mechanism would only result in a small reduction of the supercurrent below the detectable level due to a breaking-up of Cooper pairs, but not in an approximate reduction onto one of the current states [105–107]. However, given the rapid development of experiments that propose to demonstrate quantum superpositions on increasingly large scales, it appears to be only a matter of time to probe the range relevant to a test of physical reduction models.

It is important to note that no deviations from linear Schrödinger dynamics have ever been observed that could not also be explained (at least in principle) as apparent deviations due to decoherence. In fact, it would be very difficult to distinguish collapse effects from decoherence, since the large number of atoms required for the collapse mechanism to be effective also leads to strong decoherence [62,108,107]. It would therefore be necessary to isolate the system of interest extremely well from its environment, such that decoherence effects can be neglected with respect to the environment-independent localization mechanism. Even in this case it might be difficult to exclude the influence of decoherence due to, for example, thermal emission of radiation, as demonstrated in the case of fullerene and C_{70} interferometry [56,57].

This leaves physical collapse theories, at least so far, in the speculative realm, with the added difficulty of obtaining relativistic generalizations [107]. Certainly, such collapse mechanisms might be discovered in the future. However, in the absence of positive experimental evidence for such effects, and given the viable option of constructing a quantum theory consistent with all observations from the minimal formalism alone (a strategy advocated in this paper), the need for a postulated collapse effect, with free parameters tuned such as to avoid inconsistencies with the observation (or nonobservation) of superpositions, appears rather doubtful.

4. Emergence of probabilities in a relative-state framework

The question of the origin and meaning of probabilities in a relative state–type interpretation that is based solely on a deterministically evolving global quantum state, and the problem of how to consistently derive Born’s rule in such a framework, has been the subject of much discussion and criticism aimed at this type of interpretation (see, e.g., [12]). Several decoherence-unrelated proposals have been put forward in the past to elucidate the meaning of probabilities and to arrive at the Born rule in an explicit or implicit relative-state context (see, for instance, [8,128,10,129–131]). However, it is highly controversial whether these approaches are successful and represent a noncircular derivation [132,12,133]. A derivation that is only based on the non-probabilistic axioms of quantum mechanics and on elements of classical decision theory has been presented by Deutsch [131]. It was criticized by Barnum et al. [134], but was subsequently defended by other authors [135,136] and embedded into an operational framework by Saunders [137]. It is

fair to say that no decisive conclusion appears to have been reached as to the success of these derivations.

Initially, decoherence was thought to provide a natural account of the probability concept in a relative-state framework, by relating the diagonal elements of the decohered reduced density matrix to a collection of possible “events” that can be reidentified over time, and by interpreting the corresponding coefficients as relative frequencies of branches, thus leading to an interpretation of quantum probabilities as empirical frequencies [14,131]. However, as it has been pointed out before [138,5,7], this argument cannot yield a noncircular derivation of the Born rule, since the formalism (in particular, the trace operation) and interpretation of reduced density matrices presume this rule.

The solution to the problem of understanding the meaning of probabilities and of deriving Born’s rule in a relative-state framework must therefore be sought on a much more fundamental level of quantum mechanics. Since this framework presumes nothing besides the unitarily evolving state vector itself, the solution should preferably be derived solely from properties of this quantum state. However, while we would like to assign probabilities to “outcomes of measurements” on a local system (i.e., probabilities for the system to be found in a certain state), the global quantum state usually contains a high degree of environmental entanglement, i.e., there exists no state vector that could be assigned to the local system alone. Still, we obviously talk regularly of the “state of the system,” and we must therefore distinguish this notion of state from the quantum state vector itself. Following the relative-state viewpoint, the local “events” of the system (or its possible “states of the system”) are then typically identified with the relative-state components of the global state vector in the Hilbert subspace corresponding to the system.

The recent enormous advances in the field of quantum information theory, especially in the understanding of the properties and implications of quantum entanglement, have shed some light on how one might proceed. Quantum information theory has established the notion that quantum theory can be viewed as a description of what, and how much, “information” Nature is willing to proliferate. For example, a peculiar feature of quantum mechanics is that complete knowledge of the global pure bipartite quantum state $|\Psi\rangle = (|\alpha_1\rangle|\beta_1\rangle + |\alpha_2\rangle|\beta_2\rangle)/\sqrt{2}$ itself does not appear to contain information about the “absolute” state of one of the subsystems. This hints at ways how a concept of “ignorance,” and therefore of probability, may emerge directly from the quantum feature of entanglement without any classical counterpart.

This idea has recently been developed in a series of papers by Zurek [5,139,140,15], leading to a proposal for a derivation of Born’s rule (see also [141,142]). As pointed out by the present author [143,7] and made more explicit in the most recent of Zurek’s articles on this topic [15], the derivation is still based on certain assumptions that are not contained in the basic measurement-free relative-state framework of quantum mechanics. One might argue how strong these assumptions are. Zurek himself, for example, considers some of them to be “facts” and regards others as “natural” and “modest” [15]; a somewhat more critical position with respect to some of the assumptions has been assumed by the present author [143]. Granted these assumptions, however, we consider Zurek’s proposal a very promising approach towards a deeper understanding of the origin of quantum probabilities, and we shall therefore outline the basic ideas and assumptions in the following (a more detailed description and discussion of the approach can be found in [5,143,7,15]).

Zurek’s derivation is based on a particular symmetry property (referred to as “environment-assisted invariance,” or “invariance” for short) of composite quantum states, which is used to infer complete ignorance about the state of the subsystem. The derivation relies on a study of the properties of a composite entangled state and therefore intrinsically requires the decomposition of the Hilbert space into subsystems and the usual tensor-product structure. The core result to be established is the following. Given a bipartite product Hilbert space $H_{S_1} \otimes H_{S_2}$ and a completely known composite pure state in the diagonal Schmidt decomposition

$$|\Psi\rangle = (e^{i\varphi_1}|\alpha_1\rangle_1|\beta_1\rangle_2 + e^{i\varphi_2}|\alpha_2\rangle_1|\beta_2\rangle_2)/\sqrt{2}, \tag{28}$$

where the $|\alpha_i\rangle_1$ and $|\beta_i\rangle_2$ are orthonormal basis vectors that span the Hilbert spaces H_{S_1} and H_{S_2} , the probabilities of obtaining either one of the relative states $|\alpha_1\rangle_1$ and $|\alpha_2\rangle_1$ (identified with the “events” of interest to which probabilities are to be assigned [140, p. 12]; see also [143]) are equal. Given this result, generalizations to higher-dimensional Hilbert spaces and to the case of unequal absolute values of the Schmidt coefficients in Eq. (28) can be achieved in a rather straightforward way [15].

This result is established in two key steps. First, a few simple assumptions (Zurek’s “facts” [15]) are introduced that connect the global quantum state $|\Psi\rangle$, Eq. (28), to the “state of the system” S_1 . This is necessary because, as mentioned above, the global quantum state is all that the pure state-vector formalism of quantum mechanics provides for the description of a bipartite system containing entanglement. The following assumptions are made about the “state of the system” S_1 . First, this state is completely determined by the global quantum state, Eq. (28); second, it specifies all measurable properties of S_1 , including probabilities of outcomes of measurements on S_1 ; and third, unitary transformations can change it only if they act on S_1 (see [143] for a discussion of this last assumption).

Granted these three assumptions, one can show that measurable properties of S_1 can depend neither

- (1) on the phases φ_i in Eq. (28), such that we can assume the simplified form

$$|\Psi\rangle = (|\alpha_1\rangle_1|\beta_1\rangle_2 + |\alpha_2\rangle_1|\beta_2\rangle_2)/\sqrt{2} \tag{29}$$

for our purpose of discussing probabilities associated with S_1 ;

- (2) nor on whether $|\alpha_1\rangle_1$ is paired with $|\beta_1\rangle_2$ or $|\beta_2\rangle_2$, i.e., the unitary transformation acting on S_1 that changes the quantum state vector

$$|\Psi\rangle = (|\alpha_1\rangle_1|\beta_1\rangle_2 + |\alpha_2\rangle_1|\beta_2\rangle_2)/\sqrt{2} \tag{30}$$

into

$$|\Psi'\rangle = (|\alpha_2\rangle_1|\beta_1\rangle_2 + |\alpha_1\rangle_1|\beta_2\rangle_2)/\sqrt{2} \tag{31}$$

cannot have altered the state of S_1 .

In a way, result (2) already indicates a feature of ignorance about the state of S_1 , since interchanging the potential “outcomes” $|\alpha_i\rangle_1$ through local operations performed on S_1 does not change any measurable properties of S_1 and can therefore be viewed as leading to a form of “objective indifference” among these outcomes. It is important to note that this effect is crucially dependent on the feature of entanglement. In a nonentangled pure

state of the form $|\Phi\rangle = (|\phi_1\rangle + e^{i\varphi}|\phi_2\rangle)\sqrt{2}$, the phase φ must of course not be ignored (and would be measurable in a suitable interference experiment), and therefore the system described by the “swapped” state $|\Phi'\rangle = (|\phi_2\rangle + e^{i\varphi}|\phi_1\rangle)\sqrt{2}$ is clearly physically different from that represented by the original state $|\Phi\rangle$.

To make the above argument more precise, in the second key step of the derivation, the notion of probabilities of the outcomes $|\alpha_i\rangle_1$ in a measurement performed on S_1 (previously only subsummed under the general heading “measurable properties of S_1 ”) is now explicitly connected to the global state vector via an additional assumption. In [15], Zurek offers three possible choices for this assumption, of which we should quote one (see also [141]). Namely, it is assumed that the form of the Schmidt product states $|\alpha_i\rangle_1|\beta_i\rangle_2$ appearing in Eq. (28) implies that the probabilities for $|\alpha_i\rangle_1$ and $|\beta_i\rangle_2$ must be equal. Given this assumption and using result (2) above, it can be readily established [143,7,15] that the probabilities for $|\alpha_1\rangle_1$ and $|\alpha_2\rangle_1$ must be equal, thus completing the derivation.

As we have pointed out elsewhere [143], the need for the final assumption may be considered a reflection of the well-worn phrase that a transition from a nonprobabilistic theory (such as quantum mechanics solely based on deterministically evolving state vectors) to a probabilistic theory (that refers to “probabilities of outcomes of local measurements”) requires, at some stage, to “put probabilities in to get probabilities out.” However, in the quantum setting, this introduction of a probability concept has a far more objective character than in the classical case. While in the latter setting probabilities refer to subjective ignorance in spite of the existence of a well-defined state (see also Section 5), in the quantum case all that is available, namely, the global entangled quantum state, is perfectly known. The objectivity of ignorance in quantum mechanics can thus be viewed as a consequence of a form of “complementarity” between local and global observables [15] and could help explain the fundamental need for a probabilistic description in the quantum setting despite the deterministic evolution of the global state vector.

It is the great merit of Zurek’s proposal to have emphasized this objective character of quantum probabilities arising from the feature of quantum entanglement. While the precise role and importance of the assumptions entering the derivation as well as the generality of the approach (given, e.g., the focus on Schmidt decompositions) would benefit from further discussion and analysis, the approach definitely sheds an interesting and new light on the nature of quantum probabilities.

5. Objectification of observables in a relative-state framework

A characteristic feature of classical physics is the fact that the state of a system can be found out and agreed upon by many independent observers (with all of them initially completely ignorant about the state) without disturbing this state. In this sense, classical states preexist objectively, resulting in our notion of “classical reality.” In contrast, as is well known, measurements on a closed quantum system will in general alter its state—unless, of course, the observer chooses to measure, by pure luck or prior knowledge, an observable with an eigenstate that coincides with the state of the system. It is therefore impossible to regard quantum states of a closed system as existing in the way that classical states do. This raises the question of how classical reality emerges from within the quantum substrate, i.e., how observables are “objectified” in the above sense.

In a first step, the decoherence program, in particular the stability criterion and the more general formalism of the “predictability sieve” [4,46,47,14,5,7] (see also Section

2.2.4), has provided an answer to the question of why only a certain subset of the possible states in the Hilbert space of the system are actually observed. Taking into account the openness of the system and the form of the system–environment interaction is crucial in determining a set of preferred stable states of the system. This supplies an elegant and physically motivated solution to the problem of the preferred basis, an issue that has often been used to challenge the feasibility of relative-state interpretations [12,144]. Nonetheless, the problem sketched in the previous paragraph remains, as any direct measurement performed on the system would, in general, still alter the state of the system.

The important next step is therefore to realize that in most (if not all) cases observers gather information about the state of a system through indirect observations, namely, by intercepting fragments of environmental degrees of freedom that have interacted with the system in the past and thus carry information about the state of the system [47,14,145,5]. Probably the most common example for such an indirect acquisition of information is the visual registration of photons that have scattered off from the object of interest (see also Section 6.3). Similar to the case of decoherence, the recognition of the openness of quantum systems is therefore crucial. However, the role of the environment is now broadened, namely, from the selection of preferred states for the system of interest and the delocalization of local phase coherence, to the transmission of information about the state of the system. The idea is then to show how, and which, information is both redundantly and robustly stored in a large number of distinct fragments of the environment in such a way that multiple observers can retrieve this information without disturbing the state of the system, thereby achieving effective classicality of the state.

This approach has recently been developed under the labels of “environment as a witness” (i.e., the recognition of the role of the environment as a communication channel) and “quantum Darwinism” (namely, the study of what information about the system can be stably stored and proliferated by the environment) [47,14,5,140,146–149]. To explicitly quantify the degree of completeness and redundancy of information imprinted on the environment, the measure of (classical [146,147] or quantum [5,148,149]) mutual information has usually been used. Roughly speaking, this quantity represents the amount of information (expressed in terms of Shannon or von Neumann entropies) about the system S that can be acquired by measuring (a fragment of) the environment \mathcal{E} . Note that the amount of information contained in each fragment is always somewhat less [149] than the maximum information provided by the system itself (as given by the von Neumann entropy of the system).

The measure of classical mutual information is based on the choice of particular observables of S and \mathcal{E} and quantifies how well one can predict the outcome of a measurement of a given observable of S by measuring some observable on a fraction of \mathcal{E} [146,147]. The quantum mutual information $\mathcal{I}_{S,\mathcal{E}}$, used in more recent studies [5,148,149], can be viewed as a generalization of classical mutual information and is defined as $\mathcal{I}_{S,\mathcal{E}} = H(S) + H(\mathcal{E}) - H(S\mathcal{E})$, where $H(\rho) = -\text{Tr}(\rho \log \rho)$ is the von Neumann entropy. Thus $\mathcal{I}_{S,\mathcal{E}}$ measures the amount of entropy produced by destroying all correlations between S and \mathcal{E} , i.e., it quantifies the degree of correlations between S and \mathcal{E} . Results derived from these measures have thus far been found to be sufficiently robust with respect to the particular choice of measure [146,147,5,148,149], although a more detailed analysis of this issue is underway [149].

The main result of this research program has been the finding that the observable of the system that can be most completely and redundantly imprinted in many distinct subsets of

the environment coincides with the “pointer” observable selected by the system–environment interaction (i.e., by the stability criterion of decoherence) [146–149]. Conversely, most other states do not seem to be redundantly storable. Thus it suffices to probe a comparably very small fraction of the environment to infer a large amount of the maximum information about the pointer state of the system. On the other hand, if the observer tried to measure other observables on the same fragment, he would learn virtually nothing, as information about the corresponding observables of the system is not redundantly stored. Thus the “pointer” states of the system play a twofold role: They are the states least perturbed by the interaction with the environment, and they are the states that can be most easily found out, without disturbing the system, by probing environmental degrees of freedom. Since the same information about the pointer observable is stored independently in many fragments of the environment, multiple observers can measure this observable on different fragments and will automatically agree on the findings. In this sense, one can ascribe (effective) objective existence to the pointer states.

The research into the objectification of observables along the lines outlined in this section is only in its beginnings. Important aspects, such as the explicit dynamical evolution of the objectification process [147] and the role of the assumptions and definitions in the current treatments of the “objectification through redundancy” idea, are currently still under investigation, as are studies involving more detailed and realistic system–environment models. However, it should have become clear that the approach of departing from the closed-system view and of describing observations as the interception of information that is redundantly and robustly stored in the environment, represents a very promising candidate for a purely quantum-mechanical account of the emergence of classical reality from the quantum domain.

6. Decoherence in the perceptive and cognitive apparatus

If, motivated by the results of the experiments described in Section 2, we assume the universal validity of the Schrödinger equation, we immediately face two related consequences:

- (1) We ought to reconcile this assumption with our perception of definite states in the macroworld, since now there is no underlying stochastic mechanism (of whatever nature) that would select, in an objective manner, a particular “outcome” among the terms in a superposition of, say, spatially localized wave packets. There exists not only a multitude, but also interference effects between them.
- (2) Schrödinger dynamics are universal, it is reasonable (at least from a scientifically reasonable functionalist’s standpoint) to also describe observers with their perceptive and cognitive apparatuses—including even what could be grouped together under the rather vague term of “consciousness” [109–111,13]—by unitarily evolving wave functions.

Both consequences follow quite naturally from the assumption of universally exact [consequence (1)] and universally applicable [consequence (2)] Schrödinger dynamics. Quite generally, the preferred strategy would be to treat them jointly: Solving the “measurement problem,” that is, consequence (1), posed by the assumption of a purely unitary quantum theory, by applying this very theory to the observer, i.e., consequence (2). If suc-

cessful, this would lead to a “subjective” resolution of the measurement problem, i.e., to a quantum-mechanical account of why we, as observers, perceive *definite* states in *specific* bases, rather than superpositions of these states. In the opinion of this author [7] and of others (see, e.g., [3,14,112,13,5]), this would also represent a sufficient solution to the problem.

6.1. General remarks

First of all, on a rather philosophical sidenote, it is clear that the familiar concepts of the world of our experience are expressed in terms of the observed specific definite states. We do not even *have* a concept available for what a state describing a superposition of an alive and dead cat would represent, because we have never observed such a state. While such a Schrödinger cat might seem exotic, we have seen that quite analogous states are realizable in the laboratory—for example, in terms of superpositions of currents running in opposite directions in SQUIDS. As we have argued in Section 2.2.3, the only way we can access such superpositions in terms of our concepts (and not just in mathematical terms) is through the definite current states $|L\rangle$ and $|R\rangle$ that are observable as individual preferred states of the system upon measurement.

Furthermore, it is virtually indisputable that we must describe all observations in terms of physical interactions between the observed system and the observer, i.e., by means of an appropriate interaction Hamiltonian \hat{H}_{int} . Such interactions do not have to be, and usually are not, direct. For example, the probably most common type of observation involves the interception of a number of photons that have interacted with the object of interest in the past and whose state is thus entangled with the state of the object. These photons then contain indirect and redundantly coded information about the object that can be revealed without significantly disturbing the state of the object (see Section 5).

If the perception of definiteness is not introduced as an extraneous postulate, but is rather understood as emerging from the unitary quantum formalism itself when observations and observers are described in physical terms, it is inevitable that attempts have to be made to analyze the cognitive apparatus in quantum-mechanical terms. It is clear that giving such an account of subjective definiteness by referring to the physical structure of observers cannot share the mathematical compactness and exactness of axiomatically introduced rules that enforce definiteness on a fundamental level of the theory. However, it is important to note that, given the paramount role of observations in quantum mechanics (mostly owing to the fact that, in general, states do not pre-exist in a classical sense), postulating such “exact” rules is tantamount to simply avoiding a physical analysis of crucial and objective (that is, interpretation-neutral) physical processes (cf. Kent’s objections to “many-worlds” interpretations [12] and Wallace’s defense [16]).

If a purely unitary time evolution is assumed and observations are modeled as physical interactions, the conclusion of the existence of quantum-mechanical superpositions of brain states corresponding to the different “outcomes” of observations is inescapable. Individual perceptions are represented by certain neuronal resting/firing patterns in the brain (see [113,114] for more precise definitions of this relationship). As we shall discuss in the next section, superpositions of resting and firing states of a neuron are extremely sensitive to environmental decoherence, with the resting and firing states forming the robust neuronal states. These states can thus be identified with “record states” that are capable of robustly encoding information in spite of environmental interactions [14,15].

As a consequence of the practically irreversible delocalization of phase relations between these record states through entanglement with the environment, a dynamical decoupling of these states results. This process represents an objective branching process due to physical interactions between subsystems and with the environment.

The remaining question is then how to relate this objective branching to the perceived subjective “branches of consciousness,” i.e., collective memory states, or “minds” (von Neumann’s principle of the “psycho-physical parallelism” [109]). Of course, the existence (and therefore the locality) of consciousness cannot actually be *derived* from the quantum-mechanical formalism. This has led some authors to conclude that the question of the relationship between subjective experience and its physical correlates can only be fully answered through the introduction of new physical laws [114]. However, in the opinion of this and other authors (see, for example, [13,115]), it is an entirely viable (if not compelling) strategy to postulate, within the formalism, the existence of consciousness based on the empirical fact of decohering wavefunction components in neuronal processes, by associating the robust components of the global wave function labelled by the decohered neuronal states with dynamically autonomous observers [2,3,116,14,13,5,115,15].

Due to the absence of more concrete theoretical and experimental insight into the physical underpinnings of the cognitive apparatus with its associated complex entities such as the “mind,” “consciousness,” and even the comparably basic “record states,” the above brief account of how subjective definiteness may emerge from purely unitary quantum mechanics must (at least for now) remain inherently somewhat vague and nontechnical. Fortunately, however, the main points of the argument are quite independent of, say, the precise details of the structures and dynamics of the information-processing cognitive entities, since the ubiquity and effectiveness of decoherence is likely to lead to very robust results. We shall therefore turn, in the next section, to concrete estimates for decoherence rates in neurons.

6.2. *Decoherence of neuronal superpositions*

The extremely complex network of about 10^{11} interacting neurons in the brain undoubtedly comprises a major part of the cognitive machinery used for processing and storing of information obtained from sensory input. Computer models of such neuronal networks (employing a massively parallel interconnected web of “switches” that are turned on and off depending on some, typically nonlinear, activation function) can exhibit rich and complex behavior similar to that encountered in cognitive processes.² In particular, it is reasonable to identify the “record states” mentioned above with individual neurons or neuronal clusters. One might conjecture that ultimately all cognitive processes (and thus presumably also our perception of consciousness) are due to neuronal activity.

Thus the importance of a quantitative investigation of decoherence in neuronal states should be clear. Tegmark [117] has estimated decoherence rates for a superposition of a

² However, as Donald [114] has pointed out, the brain should not be thought of as a deterministic classical computer with a predictable input/output pattern, since synaptic transmissions have a fairly high failure rate due to the complexity of the underlying biological processes. The large number of about 10^{14} synapses in the human brain, with each neuron firing in average several times per second, inevitably leads to a high degree of unpredictability on the “everyday level” that is much more significant than effects due to pure quantum uncertainties.

firing and non-firing neuron in the brain. The firing is represented by a large number $N \sim 10^6$ [117] of Na^+ ions moving across the membrane into the inside of the axon (Fig. 11). Thus, a superposition of a firing and nonfiring neuron corresponds to a spatial superposition involving $O(N)$ Na^+ ions.

The extensive difference \mathcal{S}_{ext} (see Section 2.1) can then be estimated to be on the order of 10^2 – 10^3 , given by a small multiple of the thickness $h \sim 10$ nm of the axon membrane separating the inside and outside regions, relative to the size of a Na^+ ion, which is on the order of 0.1 nm. While this value for \mathcal{S}_{ext} is comparably small, the degree of entanglement \mathcal{S}_{ent} is somewhat closer to the values listed in Table 1. Taking it to be equal to the number of microscopic constituents, we obtain $\mathcal{S}_{\text{ent}} \sim 3 \times 10^7$. Thus a neuron being in a superposition of firing and resting quite clearly falls into the macroscopic category.

The decoherence rates for this superposition as estimated by Tegmark are, as expected, extremely fast. The three main sources of decoherence in this case, namely, ion-ion scattering, ion-water collisions, and long-range Coulomb interactions due to nearby ions, all result in decoherence times on the order of 10^{-20} s.

One obvious implication of fast neuronal decoherence is that coherent superpositions in neurons could never be sustained long enough to allow for some form of quantum computation. This result appears to be much more clearly established than an answer to the question of whether the relevant decoherence times are long enough to allow for quantum computation in microtubules (dynamically active structures that are a dominant part of the cytoskeleton, i.e., the internal scaffolding of cells). Suggestions in the positive,

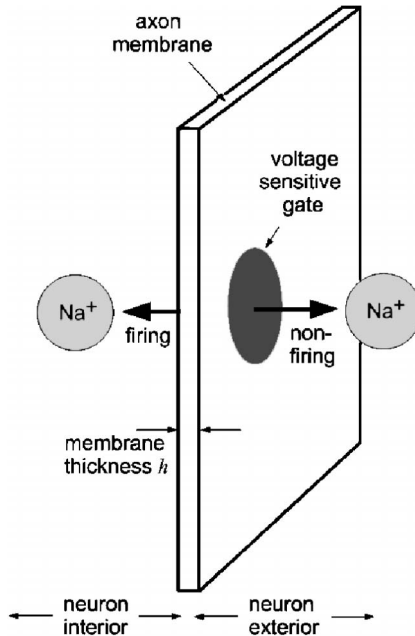


Fig. 11. Schematic illustration of the axon membrane of a neuron. The firing of the neuron corresponds to a net flow of $N \sim 10^6$ sodium ions into the inside of the axon. Superpositions of firing and non-firing neuronal states (i.e., of N ions being in a spatial superposition of inside and outside the membrane) are decohered on a time scale of about 10^{-20} s [117].

including the association of such quantum computations with the emergence of consciousness, have been put forward in [118–120], criticized in [117], subsequently defended in [121], and further evaluated in [122] (see also [123]).

However, the question much more relevant to the theme of this paper concerns the implications of neuronal decoherence for a decoherence-based account of subjective definiteness in unitary quantum mechanics—i.e., for a subjective resolution of the “measurement problem.” To this extent, let us in the following discuss a simple step-by-step quantum-mechanical account of the chain of interactions leading to the recording of a visual event in the brain.

6.3. Schematic sketch of the chain of interactions in visual perception and cognition

Suppose that a small number of photons interact with an object \mathcal{O} described by a pure-state superposition of two macroscopically distinct positions. This step already can be viewed as an environmental decoherence process, where now, however, the environment assumes a crucial role as a carrier of information (see Section 5). Due to entanglement, the combined object-photon system will be described by a superposition of the form

$$|\Psi_{\mathcal{OP}}\rangle = \frac{1}{\sqrt{2}}(|\omega_1\rangle_{\mathcal{O}}|\phi_1\rangle_{\mathcal{P}} + |\omega_2\rangle_{\mathcal{O}}|\phi_2\rangle_{\mathcal{P}}), \quad (32)$$

where ω_i , $i = 1, 2$, are the two distinct (small) spatial regions associated with the object, and $|\phi_i\rangle_{\mathcal{P}}$ denote the corresponding classically distinct collective photon states. A conceptually similar arrangement on the mesoscopic scale has explicitly been studied in experiments involving a single rubidium atom (representing the object) in a superposition of two internal levels and entangled with a cavity radiation mode (corresponding to the collection of photons) [30,31].

Initial detection of such a collection of photons in the (human) eye is associated with rhodopsin molecules in the retina. Due to their mesoscopic properties, rhodopsin molecules are subject to strong decoherence, such that already at this stage the influence of the environment will have preselected the robust states $|\rho_i\rangle_{\mathcal{R}}$ of the rhodopsin molecule, which correspond to certain photon detection events $|\phi_i\rangle_{\mathcal{P}}$. The total state $|\Psi_{\mathcal{OPR}}\rangle$ will then be given by

$$|\Psi_{\mathcal{OPR}}\rangle = \frac{1}{\sqrt{2}}(|\omega_1\rangle_{\mathcal{O}}|\phi_1\rangle_{\mathcal{P}}|\rho_1\rangle_{\mathcal{R}} + |\omega_2\rangle_{\mathcal{O}}|\phi_2\rangle_{\mathcal{P}}|\rho_2\rangle_{\mathcal{R}}), \quad (33)$$

i.e., the photon–rhodopsin interaction should lead to an (albeit, due to the influence of decoherence, very fragile) superposition of the different biochemically distinct states $|\rho_i\rangle_{\mathcal{R}}$ of the rhodopsin molecule.³ These relative states can then be expected to be further correlated with the appropriate states $|v_i\rangle_{\mathcal{N}}$ of neuronal arrays that are mainly located in the primary visual area in the occipital lobe of the brain. Suppose that the two “events” represented by the two distinct states $|\rho_i\rangle_{\mathcal{R}}$ of the rhodopsin molecule (corresponding to the different photon states $|\phi_i\rangle_{\mathcal{P}}$ that in turn carry information about the two distinct spatial regions ω_i of the object) are encoded by the states $|v_i\rangle_{\mathcal{N}}$,

³ A search for experimental evidence for such superpositions has been suggested in [124]; for an experimental proposal, see [125]. Cf. also [126] for an (unconvincing) suggestion that the visual apparatus itself might trigger a physical collapse.

$i = 1, 2$, describing the same collection of N neurons in two different firing/resting patterns.

As a simple example, let us take $N = 3$, and $|v_1\rangle_{\mathcal{N}} = |1\rangle_{\mathcal{N}_1}|0\rangle_{\mathcal{N}_2}|1\rangle_{\mathcal{N}_3}$ and $|v_2\rangle_{\mathcal{N}} = |0\rangle_{\mathcal{N}_1}|1\rangle_{\mathcal{N}_2}|1\rangle_{\mathcal{N}_3}$, where $|0\rangle_{\mathcal{N}_i}$ and $|1\rangle_{\mathcal{N}_i}$ denote, respectively, the resting and firing state of the i th neuron. Then the combined state $|\Psi_{OPRN}\rangle$ will be given by

$$|\Psi_{OPRN}\rangle = \frac{1}{\sqrt{2}}(|\omega_1\rangle_{\mathcal{O}}|\phi_1\rangle_{\mathcal{P}}|\rho_1\rangle_{\mathcal{R}}|1\rangle_{\mathcal{N}_1}|0\rangle_{\mathcal{N}_2}|1\rangle_{\mathcal{N}_3} + |\omega_2\rangle_{\mathcal{O}}|\phi_2\rangle_{\mathcal{P}}|\rho_2\rangle_{\mathcal{R}}|0\rangle_{\mathcal{N}_1}|1\rangle_{\mathcal{N}_2}|1\rangle_{\mathcal{N}_3}). \quad (34)$$

The extreme fast decoherence rate for the neurons 1 and 2 being in a superposition of firing and resting will lead to a practically irreversible dynamical decoupling of the two branches that now describe two distinct “outcomes” encoded by $|v_i\rangle_{\mathcal{N}}$. We may then identify these states with the basic memory states, although, strictly speaking, the physical process of actual information storage in the brain (i.e., learning) occurs only in two subsequent stages [127]. First, in form of short-term memory, believed to be due to certain biochemical and electrical interactions between neurons. Second, as long-term memory that is based on actual structural changes in the brain (“neuroplasticity”), most notably, due to the formation of new connections (synapses) between neurons and due to internal changes in the synaptic regions in individual neurons.

However, since all these processes will again be subject to strong decoherence, the essence of our argument is not altered: The states in a superposition of neuronal firing patterns will rapidly entangle with approximately orthogonal (i.e., macroscopically distinguishable) states of the environment and thus lead to the formation of locally noninterfering (that is, dynamically autonomous) branches labelled by these “outcome” states. Regardless of the precise physical, chemical, biological, psychological, etc., details of perceptive and cognitive activity, it is quite clear that decoherence effects are likely to be sufficient to explain the emergence of a subjective perception of single outcomes, represented by stable, “classical,” record states, from a (by all accounts macroscopic) global superposition.

7. Discussion and outlook

We have analyzed three important experimental domains—namely, SQUIDs, molecular diffraction, and Bose–Einstein condensation—that have demonstrated (or at least have come very close to demonstrating) the existence of superpositions of states that can be considered macroscopically distinct in comparison with the microscopic states “typically” treated in quantum mechanics. These experiments have provided powerful examples for the validity of unitary Schrödinger dynamics and the superposition principle on increasingly large length scales. They have also shown how the fragility of macroscopic superpositions can be precisely understood and controlled in terms of environmental interactions and the resulting decoherence effects.

Of course, these experiments do not *falsify* the possibility that the Schrödinger equation might not be exact under all circumstances. In fact, no finite number of experiments that show the validity of unitary dynamics could ever do. To do so, a “positive-test” experiment would be needed that could explicitly demonstrate nonlinear deviations from the Schrödinger equation. Leggett [34,32] has presented a Bell-type inequality that would be obeyed by what he calls the class of “macrorealistic theories,” while it would be violated

by the predictions of purely unitary quantum mechanics. The “macrorealistic” class is defined to represent all theories in which macroscopic systems are always in a single definite state among a collection of possible macroscopically distinct states, and in which this definite state can be found out without perturbing the state and dynamics of the system. So one might, at least in principle, through suitable experiments be able to exclude either any such macrorealistic theory or the universal validity of the Schrödinger equation. Such a strategy would be similar in spirit to the tests of Bell’s inequalities, which rule out a large class of, if not all, local realistic theories. (See Section 6 of [32] and references therein for some first ideas in this direction.)

At the current stage, however, it is the opinion of the present author that, in absence of any positive evidence for deviations from unitary dynamics, combined with the continued experimental verification of increasingly large “Schrödinger cats” (whose time evolution, including decoherence effects, is in perfect agreement with unitary dynamics), it appears to be not only reasonable, but moreover compelling, to entertain the possibility of a universally exact Schrödinger equation seriously and to fully explore the consequences of this assumption.

The experiments described in this paper have demonstrated rapid progress in achieving, controlling, and observing superpositions of increasingly distinct states. Experiments involving superpositions of classically distinguishable states of a few photons [30,31] have been followed by collective superpositions of 10^9 electron pairs in SQUIDS and double slit-type experiments using massive molecules with a large number of degrees of freedom. It is only a matter of time until number-difference superpositions involving on the order of 10^7 rubidium atoms will be experimentally realized in BECs. It is rather unlikely that this progress towards experimental evidence for increasingly large superpositions will encounter any fundamental boundaries in the near future. As we have seen, the main limit seems to be given by the ability to shield the system sufficiently from the decohering influence of the environment. This limit is open to precise quantitative analysis.

In view of this situation, we may now legitimately ask what the next steps in solidifying the empirical support for a purely unitary quantum theory and its consequences might ideally look like. To this extent, we remark that superpositions of macroscopically distinct states that refer to biological (and, even more so, animate) objects seem to have been considered as particular “paradoxical”—after all, Schrödinger chose a cat to illustrate his famous *Gedanken* experiment. This attitude may be traced back to several reasons. For example:

- (1) The “distinctness” between the states referring to biological objects is usually extremely complex. Not only is the number of physical, chemical, biological, etc., differences between a dead and alive cat overwhelmingly vast, even two functionally different states of a simple biological molecule will be distinct in a large number of features. By contrast, in the examples involving inanimate objects, such as BECs and SQUIDS, the states in the superposition usually differ only in a single physical quantity, such as total angular momentum or magnetic moment.
- (2) While we might be willing to accept the existence of an “exotic” superposition under extreme physical conditions (such as superconducting currents in a bulk of matter cooled down to temperatures close to absolute zero), biological objects reside in the parameter regime characteristic of the world of our everyday experience.

- (3) If the superposition principle is applied to human observers (specifically, superpositions of “states of consciousness,” etc.), we feel that our most basic intuition about possessing a unique identity has been infringed upon.

Especially in light of the first two arguments, the molecular diffraction experiments appear to be the most “natural” realization of superpositions of macroscopically distinct states. In fact, as pointed out in Section 2.3.2, interference effects have already been experimentally demonstrated for a biological molecule [51], and larger biological structures are likely to follow [52,55] (see also Fig. 9).

However, another interesting direction could also be taken from here. As suggested for example in [124,32], one might try to look for interference effects between (and thus superpositions of) *biologically* distinct states of the same biomolecule, rather than for the spatial superpositions demonstrated in the current molecular-diffraction setups. While such experiments would be considerably more difficult to carry out due to the required near-in vivo environmental conditions (room temperatures, presence of a surrounding medium such as an aqueous solution, etc.), which would lead to very strong decoherence effects, there does not seem to exist a fundamental obstacle that would prevent one in principle from the realization of such superpositions in a cleverly designed setup.

Experiments that would find some basic biological structure in a superpositions of distinct states corresponding to different biological “inputs” might in turn indicate the presence of a superposition of input signals originating from the inanimate outside world (e.g., a superposition of photon states entangled with spatially distinct states of a single object—see Section 6.3). They could also provide direct empirical evidence for consequences of purely unitary quantum mechanics in the regime of more complex structures that are part of conscious (human) observers, and might therefore also ease the discomfort spelled out in item (3) above.

Given that experiments [51] have demonstrated a splitting of the localized state of a biomolecule into “branches” corresponding to distinct paths, it would also be worth discussing, as Zeh [13] puts it,

the consequences of similar *Gedanken* experiments with objects carrying some primitive form of “core consciousness”—including an elementary awareness of their path through the slits.

In such a situation, after passage through the slits, the state of the object would be described by a superposition of spatially distinct trajectories. However, due to its awareness of the path, it would thus also be in a superposition of multiple (local) “states of consciousness.” Environmental scattering would then lead to entanglement with path-encoding variables (decoherence), which hence would also destroy interference effects between the “branches of consciousness,” and thus the different paths would be “experienced” separately. In the absence of decoherence, it would be possible to coherently recombine the branches into a single localized wavepacket identical to the state before the passage through the slits. It then follows from the standard quantum-mechanical formalism that the associated object then cannot have retained any “memory” of the path taken before the recombination. For related ideas using the example of neutron interferometry, see [19].

As it is well known, Bohr has repeatedly insisted on the fundamental role of classical concepts (see, for example, [150,151]). The experimental evidence for superpositions of

macroscopically distinct states on increasingly large length scales counters such a dictum. Superpositions appear to be novel and individually existing states, often without any classical counterparts. Only the physical interactions between systems then determine a particular decomposition into classical states from the view of each particular system. Thus classical concepts are to be understood as locally emergent in a relative-state sense and should no longer claim a fundamental role in the physical theory.

We have already widely acknowledged, based on experimental evidence, the fundamental nonlocality of the quantum world, in spite of the utterly nonclassical implications. We also have obtained direct evidence for the validity of unitary dynamics and the superposition principle in all experiments conducted so far, although this has forced us to again accept extremely nonclassical situations as physical reality. Why not let these experiences guide us to extend our willingness to entirely give up classical prejudice and instead explore the consequences of a strictly unitary quantum theory embedded into a minimal interpretive framework? After all, exploring the implications of pure quantum features to the largest possible extent can in turn give us back the familiar “classical” notions of the world of our experience. As we have discussed in this paper, consequences of highly nonlocal quantum entanglement lead to the local disappearance of quantum interference effects, may explain the origin of probabilities in quantum mechanics, and are likely capable of accounting for the objectification of observables and therefore the emergence of effective classical reality, thus supplying the missing pieces of the basic Everett theory that have frequently been used to challenge the viability of a relative state-type “minimal interpretation.”

Acknowledgments

The author thanks A. Fine and H.D. Zeh for fruitful discussions and helpful comments.

References

- [1] E. Schrödinger, *Naturwissenschaften* 23 (1935) 807–812, 823–828, 844–849.
- [2] H.D. Zeh, *Found. Phys.* 1 (1970) 69–76.
- [3] H.D. Zeh, *Found. Phys.* 3 (1973) 109–116.
- [4] W.H. Zurek, *Phys. Rev. D* 24 (1981) 1516–1525.
- [5] W.H. Zurek, *Rev. Mod. Phys.* 75 (2003) 715–775.
- [6] E. Joos, H.D. Zeh, C. Kiefer, D. Giulini, J. Kupsch, I.-O. Stamatescu, *Decoherence and the Appearance of a Classical World in Quantum Theory*, second ed., Springer, New York, 2003.
- [7] M. Schlosshauer, *Rev. Mod. Phys.* 76 (2004) 1267–1305.
- [8] H. Everett, *Rev. Mod. Phys.* 29 (1957) 454–462.
- [9] B.S. DeWitt, *Phys. Today* 23 (1970) 30–35.
- [10] B.S. DeWitt, in: B. d’Espagnat (Ed.), *Foundations of Quantum Mechanics*, Academic Press, New York, 1971, pp. 211–262.
- [11] B.S. DeWitt, N. Graham, *The Many-Worlds Interpretation of Quantum Mechanics*, Princeton University, Princeton, 1973.
- [12] A. Kent, *Int. J. Mod. Phys. A* 5 (1990) 1745.
- [13] H.D. Zeh, *Found. Phys. Lett.* 13 (2000) 221–233.
- [14] W.H. Zurek, *Philos. Trans. R. Soc. Lond. Ser. A* 356 (1998) 1793–1821.
- [15] W.H. Zurek, Available from: <quant-ph/0405161/>.
- [16] D. Wallace, *Stud. Hist. Philos. Mod. Phys.* 34 (2003) 87–105.
- [17] D. Wallace, *Stud. Hist. Philos. Mod. Phys.* 33 (2002) 637–661.
- [18] D. Deutsch, *Int. J. Theor. Phys.* 24 (1985) 1–41.

- [19] L. Vaidman, *Int. Stud. Philos. Sci.* 12 (1998) 245–261.
- [20] M.J. Donald, Available from: <quant-ph/9904001/>.
- [21] J. Clarke, A.N. Cleland, M.H. Devoret, D. Esteve, J.M. Martinis, *Science* 239 (1988) 992–997.
- [22] R. Rouse, S. Han, J.E. Lukens, *Phys. Rev. Lett.* 75 (1995) 1614–1617.
- [23] P. Silvestrini, V.G. Palmieri, B. Ruggiero, M. Russo, *Phys. Rev. Lett.* 79 (1997) 3046–3049.
- [24] R. Rouse, S. Han, J.E. Lukens, in: G.D. Palazzi, C. Cosmelli, L. Zanello (Eds.), *Phenomenology of Unification from Present to Future*, World Scientific, Singapore, 1998, pp. 207–224.
- [25] Y. Nakamura, Y.A. Pashkin, J.S. Tsai, *Nature* 398 (1999) 786–788.
- [26] J.R. Friedman, M.P. Sarachik, J. Tejada, R. Ziolo, *Phys. Rev. Lett.* 76 (1996) 3830–3833.
- [27] W. Wernsdorfer, E.B. Orozco, K. Hasselbach, A. Benoit, D. Mailly, O. Kubo, H. Nakano, B. Barbara, *Phys. Rev. Lett.* 79 (1997) 4014–4017.
- [28] E.D. Barco, N. Vernier, J.M. Hernández, J. Tejada, E.M. Chudnovsky, E. Molins, G. Bellessa, *Europhys. Lett.* 47 (1999) 722–728.
- [29] C. Monroe, D.M. Meekhof, B.E. King, D.J.A. Wineland, *Science* 272 (1996) 1131–1136.
- [30] M. Brune, E. Hagley, J. Dreyer, X. Maître, A. Maali, C. Wunderlich, J.M. Raimond, S. Haroche, *Phys. Rev. Lett.* 77 (1996) 4887–4890.
- [31] J.M. Raimond, M. Brune, S. Haroche, *Phys. Rev. Lett.* 79 (1997) 1964–1967.
- [32] A.J. Leggett, *J. Phys.: Condens. Matter* 14 (2002) R415–R451.
- [33] D.M. Greenberger, M.A. Horne, A. Shimony, A. Zeilinger, *Am. J. Phys.* 58 (1990) 1131–1143.
- [34] A.J. Leggett, *Suppl. Prog. Theor. Phys.* 69 (1980) 80–100.
- [35] U. Weiss, *Quantum Dissipative Systems*, World Scientific, Singapore, 1999.
- [36] P. Silvestrini, B. Ruggiero, Y.N. Ovchinnikov, *Phys. Rev. B* 54 (1996) 1246–1250.
- [37] C.H. van der Wal, A.C.J. ter Haar, F.K. Wilhelm, R.N. Schouten, C.J.P.M. Harmans, T.P. Orlando, S. Lloyd, J.E. Mooij, *Science* 290 (2000) 773–777.
- [38] J.R. Friedman, V. Patel, W. Chen, S.K. Yalpygo, J.E. Lukens, *Nature* 406 (2000) 43–46.
- [39] M.J. Everitt, T.D. Clark, P.B. Stiffell, A. Vourdas, J.F. Ralph, R.J. Prance, H. Prance, *Phys. Rev. A* 69 (2004) 043804.
- [40] A.N. Korotkov, D.V. Averin, *Phys. Rev. B* 64 (2001) 165310.
- [41] A.N. Korotkov, *Phys. Rev. B* 63 (2001) 115403.
- [42] Y.S. Greenberg, A. Izmalkov, M. Grajcar, E. Ilichev, W. Krech, H.-G. Meyer, *Phys. Rev. B* 66 (2002) 224511.
- [43] J.M. Martinis, S. Nam, J. Aumentado, C. Urbina, *Phys. Rev. Lett.* 89 (2002) 117901.
- [44] Y. Yu, S. Han, X. Chu, S.-I. Chu, Z. Wang, *Science* 296 (2002) 889–892.
- [45] D. Vion, A. Aassime, A. Cottet, P. Joyez, H. Pothier, C. Urbina, D. Esteve, M.H. Devoret, *Science* 296 (2002) 886–889.
- [46] W.H. Zurek, *Phys. Rev. D* 26 (1982) 1862–1880.
- [47] W.H. Zurek, *Prog. Theor. Phys.* 89 (1993) 281–312.
- [48] E.M. Chudnovsky, A.B. Kuklov, *Phys. Rev. B* 67 (2003) 064515.
- [49] M. Arndt, O. Nairz, J. Vos-Andreae, C. Keller, G. van der Zouw, A. Zeilinger, *Nature* 401 (1999) 680–682.
- [50] B. Brezger, L. Hackermüller, S. Uttenthaler, J. Petschinka, M. Arndt, A. Zeilinger, *Phys. Rev. Lett.* 88 (2002) 100404.
- [51] L. Hackermüller, S. Uttenthaler, K. Hornberger, E. Reiger, B. Brezger, A. Zeilinger, M. Arndt, *Phys. Rev. Lett.* 91 (2003) 090408.
- [52] M. Arndt, O. Nairz, A. Zeilinger, in: R.A. Bertlmann, A. Zeilinger (Eds.), *Quantum [Un]Speakables: From Bell to Quantum Information*, Springer, Berlin, 2002, pp. 333–351.
- [53] O. Nairz, M. Arndt, A. Zeilinger, *Am. J. Phys.* 71 (2003) 317–325.
- [54] K. Hornberger, S. Uttenthaler, B. Brezger, L. Hackermüller, M. Arndt, A. Zeilinger, *Phys. Rev. Lett.* 90 (2003) 160401.
- [55] L. Hackermüller, K. Hornberger, B. Brezger, A. Zeilinger, M. Arndt, *Appl. Phys. B* 77 (2003) 781–787.
- [56] L. Hackermüller, K. Hornberger, B. Brezger, A. Zeilinger, M. Arndt, *Nature* 427 (2004) 711–714.
- [57] K. Hornberger, L. Hackermüller, M. Arndt, *Phys. Rev. A* 71 (2005) 023601.
- [58] C.J. Bordé, N. Courtier, F. du Burck, A.N. Goncharov, M. Gorlicki, *Phys. Lett. A* 188 (1994) 187–197.
- [59] M.S. Chapman, C.R. Ekstrom, T.D. Hammond, R.A. Rubenstein, J. Schmiedmayer, S. Wehinger, D.E. Pritchard, *Phys. Rev. Lett.* 74 (1995) 4783–4786.
- [60] E. Joos, H.D. Zeh, *Z. Phys. B: Condens. Matter* 59 (1985) 223–243.
- [61] M.R. Gallis, G.N. Fleming, *Phys. Rev. A* 42 (1990) 38–48.

- [62] M. Tegmark, *Found. Phys. Lett.* 6 (1993) 571–590.
- [63] K. Hornberger, J.E. Sipe, *Phys. Rev. A* 68 (2003) 012105.
- [64] K. Hornberger, J.E. Sipe, M. Arndt, *Phys. Rev. A* 70 (2004) 053608.
- [65] M.R. Andrews, C.G. Townsend, H.-J. Miesner, D.S. Durfee, D.M. Kurn, W. Ketterle, *Science* 275 (1997) 637–641.
- [66] Y. Shin, M. Saba, T.A. Pasquini, W. Ketterle, D.E. Pritchard, A.E. Leanhardt, *Phys. Rev. Lett.* 92 (2004) 050405.
- [67] A. Einstein, *Sitzungsber. Preuss. Akad. Wiss.* 22 (1924) 261–267.
- [68] A. Einstein, *Sitzungsber. Preuss. Akad. Wiss.* 1 (1925) 3–14.
- [69] A. Einstein, *Sitzungsber. Preuss. Akad. Wiss.* 3 (1925) 18–25.
- [70] S.N. Bose, *Z. Phys.* 26 (1924) 178–181.
- [71] C.C. Bradley, C.A. Sackett, J.J. Tollet, R. Hulet, *Phys. Rev. Lett.* 75 (1995) 1687–1690.
- [72] K.B. Davis, M.-O. Mewes, M.R. Andrews, N.J. van Druten, D.S. Durfee, D.M. Kurn, W. Ketterle, *Phys. Rev. Lett.* 75 (1995) 3969–3973.
- [73] M.H. Anderson, J.R. Ensher, M.R. Matthews, C.E. Wieman, E.A. Cornell, *Science* 269 (1995) 198–201.
- [74] C.C. Bradley, C.A. Sackett, R. Hulet, *Phys. Rev. Lett.* 78 (1997) 985–989.
- [75] J. Javanainen, S.M. Yoo, *Phys. Rev. Lett.* 76 (1996) 161–164.
- [76] A. Röhrl, M. Naraschewski, A. Schenzle, H. Wallis, *Phys. Rev. Lett.* 78 (1997) 4143–4146.
- [77] J. Javanainen, *Science* 307 (2005) 1883–1885.
- [78] M. Saba, T.A. Pasquini, C. Sanner, Y. Shin, W. Ketterle, D.E. Pritchard, *Science* 307 (2005) 1945–1948.
- [79] L.A. Collins, L. Pezze, A. Smerzi, G.P. Berman, A.R. Bishop, *Phys. Rev. A* 71 (2005) 033628.
- [80] J.I. Cirac, M. Lewenstein, K. Mølmer, P. Zoller, *Phys. Rev. A* 57 (1998) 1208–1218.
- [81] J. Ruostekoski, M.J. Collett, R. Graham, D.F. Walls, *Phys. Rev. A* 57 (1998) 511–517.
- [82] D. Gordon, C.M. Savage, *Phys. Rev. A* 59 (1999) 4623–4629.
- [83] J.A. Dunningham, K. Burnett, *J. Mod. Opt.* 48 (2001) 1837–1853.
- [84] J. Calsamiglia, M. Mackie, K.-A. Suominen, *Phys. Rev. Lett.* 87 (2001) 160403.
- [85] P.J.Y. Louis, P.M.R. Brydon, C.M. Savage, *Phys. Rev. A* 64 (2001) 053613.
- [86] A. Micheli, D. Jaksch, J.I. Cirac, P. Zoller, *Phys. Rev. A* 67 (2003) 013601.
- [87] J. Ruostekoski, D.F. Walls, *Phys. Rev. A* 58 (1998) R50–R53.
- [88] L.-M. Kuang, Z.-Y. Tong, Z.-W. Ouyang, H.-S. Zeng, *Phys. Rev. A* 61 (1999) 013608.
- [89] D.A.R. Dalvit, J. Dziarmaga, W.H. Zurek, *Phys. Rev. A* 62 (2000) 013607.
- [90] M.W. Jack, M. Yamashita, *Phys. Rev. A* 71 (2005) 033619.
- [91] K.W. Mahmud, M.A. Leung, W.P. Reinhardt, Available from: <cond-mat/0403002/>.
- [92] K.W. Mahmud, H. Perry, W.P. Reinhardt, *Phys. Rev. A* 71 (2005) 023615.
- [93] A. Polkovnikov, S. Sachdev, S.M. Girvin, *Phys. Rev. A* 66 (2002) 053607.
- [94] A. Polkovnikov, *Phys. Rev. A* 68 (2003) 033609.
- [95] N.D. Mermin, *Phys. Rev. Lett.* 65 (1990) 3373–3376.
- [96] C.A. Sackett, D. Kielpinski, B.E. King, C. Langer, V. Meyer, C.J. Myatt, M. Rowe, Q.A. Turchette, W.M. Itano, D.J. Wineland, C. Monroe, *Nature* 404 (2000) 256–259.
- [97] M. Albiez, R. Gati, J. Fölling, S. Hunsmann, M. Cristiani, M.K. Oberthaler, Available from: <cond-mat/0411757/>.
- [98] J.S. Bell, *Found. Phys.* 12 (1982) 989–999.
- [99] P. Pearle, *Phys. Rev. A* 39 (1989) 2277–2289.
- [100] L. Diósi, *Phys. Rev. A* 40 (1989) 1165–1174.
- [101] G.C. Ghirardi, P. Pearle, A. Rimini, *Phys. Rev. A* 42 (1990) 78–89.
- [102] S.L. Adler, *Quantum Theory as an Emergent Phenomenon*, Cambridge University, Cambridge, England, 2004, Ch. 6.5.
- [103] W. Marshall, C. Simon, R. Penrose, D. Bouwmeester, *Phys. Rev. Lett.* 91 (2003) 130401.
- [104] A. Bassi, E. Ippoliti, S.L. Adler, *Phys. Rev. Lett.* 94 (2005) 030401.
- [105] A.I.M. Rae, *J. Phys. A* 23 (1990) L57–L60.
- [106] M. Buffa, O. Nicrosini, A. Rimini, *Found. Phys. Lett.* 8 (1995) 105–125.
- [107] A. Bassi, G.C. Ghirardi, *Phys. Rep.* 379 (2003) 257–426.
- [108] F. Benatti, G.C. Ghirardi, R. Grassi, in: E.G. Beltrametti, J.-M. Lévy-Leblond (Eds.), *Advances in Quantum Phenomena*, Plenum, New York, 1995, pp. 263–279.
- [109] J. von Neumann, *Mathematische Grundlagen der Quantenmechanik*, Springer, Berlin, 1932.

- [110] E.P. Wigner, in: I.J. Good (Ed.), *The Scientist Speculates: An Anthology of Partly-Baked Ideas*, Heinemann, London, 1962.
- [111] H.P. Stapp, *Mind, Matter, and Quantum Mechanics*, first ed., Springer, New York, 1993.
- [112] B. d'Espagnat, *Phys. Lett. A* 282 (2000) 133–137.
- [113] M.J. Donald, *Found. Phys.* 25 (1995) 529–571.
- [114] M.J. Donald, Available from: <quant-ph/0208033/>.
- [115] H.D. Zeh, in: J.D. Barrow, P.C.W. Davies, C.L. Harper (Eds.), *Science and Ultimate Reality: Quantum Theory, Cosmology and Complexity*, Cambridge University Press, Cambridge, MA, 2004, pp. 103–120.
- [116] M. Lockwood, *Br. J. Philos. Sci.* 47 (1996) 159–188.
- [117] M. Tegmark, *Phys. Rev. E* 61 (2000) 4194–4206.
- [118] R. Penrose, *Shadows of the Mind*, Oxford University Press, New York, 1994.
- [119] S.R. Hameroff, R. Penrose, in: S.R. Hameroff, A.K. Kasszniak, A.C. Scott (Eds.), *Toward a Science of Consciousness—The First Tucson Discussions and Debates*, MIT Press, Cambridge, 1996, pp. 507–540.
- [120] S. Hameroff, R. Penrose, *J. Conscious. Stud.* 3 (1996) 36–53.
- [121] S. Hagan, S.R. Hameroff, J.A. Tuszynski, *Phys. Rev. E* 65 (2002) 061901.
- [122] L.P. Rosa, J. Faber, *Phys. Rev. E* 70 (3) (2004) 031902.
- [123] H.P. Stapp, Available from: <quant-ph/0010029/>.
- [124] A. Shimony, in: R.A. Healey, G. Hellman (Eds.), *Quantum Measurement: Beyond Paradox*, University of Minnesota, Minneapolis, 1998.
- [125] P.S. Hilaire, D. Bierman, S. Hameroff, Quantum states in the retina?, <http://www.quantumconsciousness.org/views/QuantumStatesRetina.html> (2002).
- [126] F.H. Thaheld, *Biosystems* 81 (2005) 113–124.
- [127] E.R. Kandel, J.H. Schwartz, T.M. Jessell, *Principles of Neural Science*, fourth ed., McGraw–Hill, New York, 2001.
- [128] J.B. Hartle, *Am. J. Phys.* 36 (1968) 704–712.
- [129] N. Graham, in: B.S. DeWitt, N. Graham (Eds.), *The Many-Worlds Interpretation of Quantum Mechanics*, Princeton University, Princeton, 1973, pp. 229–253.
- [130] R. Geroch, *Noûs* 18 (1984) 617–633.
- [131] D. Deutsch, *Proc. R. Soc. Lond. Ser. A* 455 (1999) 3129–3197.
- [132] H. Stein, *Noûs* 18 (1984) 635–652.
- [133] E.J. Squires, *Phys. Lett. A* 145 (1990) 67–68.
- [134] H. Barnum, C.M. Caves, J. Finkelstein, C.A. Fuchs, R. Schack, *Proc. R. Soc. Lond. Ser. A* 456 (2000) 1175–1182.
- [135] R.D. Gill, in: M. Schürmann, U. Franz (Eds.), *Quantum Probability and Infinite Dimensional Analysis: From Foundations to Applications*, World Scientific, Singapore, (in press), Available from: <quant-ph/0307188/>.
- [136] D. Wallace, *Stud. Hist. Philos. Mod. Phys.* 34 (2003) 415–439.
- [137] S. Saunders, Available from: <quant-ph/0211138/>.
- [138] H.D. Zeh, in: M. Ferrero, A. van der Merwe (Eds.), *New Developments on Fundamental Problems in Quantum Physics (Oviedo II)*, Kluwer Academic, Dordrecht, 1997, pp. 441–452.
- [139] W.H. Zurek, *Phys. Rev. Lett.* 90 (2003) 120404.
- [140] W.H. Zurek, in: J.D. Barrow, P.C.W. Davies, C.H. Harper (Eds.), *Science and Ultimate Reality: Quantum Theory, Cosmology and Complexity*, Cambridge University, Cambridge, England, 2004, pp. 121–137.
- [141] H. Barnum, Available from: <quant-ph/0312150/>.
- [142] U. Mohrhoff, *Int. J. Quantum Inf.* 2 (2004) 221–230.
- [143] M. Schlosshauer, A. Fine, *Found. Phys.* 35 (2005) 197–213.
- [144] H.P. Stapp, *Can. J. Phys.* 80 (2002) 1043–1052.
- [145] W.H. Zurek, *Ann. Phys. (Leipzig)* 9 (2000) 855–864.
- [146] H. Ollivier, D. Poulin, W.H. Zurek, *Phys. Rev. Lett.* 93 (2004) 220401.
- [147] H. Ollivier, D. Poulin, W.H. Zurek, Available from: <quant-ph/0408125/>.
- [148] R. Blume-Kohout, W.H. Zurek, Available from: <quant-ph/0408147/>.
- [149] R. Blume-Kohout, W.H. Zurek, Available from: <quant-ph/0505031/>.
- [150] N. Bohr, *Z. Physik* 13 (1923) 117–165.
- [151] N. Bohr, *Dialectica* 2 (1948) 312–319.